Fermi National Accelerator Laboratory

Fermilab-Pub-85/152-T
October, 1985.

QCD RADIATIVE CORRECTIONS TO PARTON PARTON SCATTERING

R. K. Ellis
and
J. C. Sexton

Fermi National Accelerator Laboratory
P. O. Box 500, Batavia, IL 60510

ABSTRACT

We present the matrix elements squared for all $(2 \to 2)$ and $(2 \to 3)$ parton scattering subprocesses calculated at $O(\alpha_S{}^3)$. The matrix elements are presented in n dimensions to regulate singularities due to the emission of soft or collinear radiation. We use these results to discuss one hadron inclusive scattering, considering only a limited number of parton subprocesses. A preliminary analysis is made of the implications of our results for gluon gluon scattering in the absence of quarks.

Operated by Universities Research Association Inc. under contract with the United States Department of Energy

The calculation of the strong radiative corrections to the parton parton scattering processes responsible for two jet structure in hadron hadron collisions was begun several years ago. Two groups (Ellis, Furman, Haber and Hinchliffe[1] and Słomiński and Furmański[2,3]) independently calculated the gluonic radiative corrections to the scattering of two non-identical quarks in order $O(\alpha_S{}^3)$. Using these results it was found that the inclusion of the $O(\alpha_S{}^3)$ terms substantially modified the naive estimate for the one particle inclusive cross-section in the kinematic region where the quark-quark scattering diagram dominates.

These papers have two shortcomings, which have become more troubling in the period since their publication. Six years ago the highest energy experiments on hadron hadron scattering were conducted at the ISR. At those energies the one particle inclusive cross-sections are dominated at large transverse momentum by quark-quark scattering because of the stiffness of the valence quark distributions in the protons. It was in this experimental scenario that the calculations of refs.[1 – 3] were meant to be applied. At the energies of the present $p\bar{p}$ colliders gluons inside hadrons cannot be neglected except at the very largest values of p_T. Indeed at super-collider energies gluons will play a pre-eminent role[4]. It is therefore a matter of some urgency to calculate the complete $O(\alpha_S{}^3)$ cross-section for all possible parton parton interactions. This is the subject of this paper.

Specifically, we present results for the invariant matrix elements squared of the following parton sub-processes in $O(\alpha_S{}^3)$.

$$
\begin{array}{lll}
(a) & q_j + q_k \to q_j + q_k & j \neq k \\
(b) & q_j + q_j \to q_j + q_j & \\
(c) & q_j + \bar{q}_j \to g + g & \\
(d) & g + g \to g + g &
\end{array}
$$

and

$$
\begin{array}{lll}
(A) & q_j + q_k \to q_j + q_k + g & j \neq k \\
(B) & q_j + q_j \to q_j + q_j + g & \\
(C) & q_j + \bar{q}_j \to g + g + g & \\
(D) & g + g \to g + g + g &
\end{array}
$$

All other matrix elements for parton parton scattering processes in $O(\alpha_S{}^3)$ can be obtained from the above by time reversal and crossing. The results are given for massless quarks and in n dimensions in order to regulate divergences.

Because the Feynman graph calculations which we have performed are complicated, we have chosen to present the full answers for all the matrix elements squared. We have taken pains also to provide sufficient detail of the methods and conventions which we adopted, so that the results which we present may be used as the input for further studies.

The second shortcoming of refs.[1 – 3] is that the calculations are performed for one particle inclusive cross-sections whereas the cross-sections of most current interest are calorimetric jet cross-sections defined in terms of the energy deposited inside a given solid angle. Such jet cross-sections are sensitive both experimentally and theoretically to the method of definition of the jet. Theoretically the sensitivity to the jet definition is present only after the inclusion of the radiative corrections calculated in this paper. The QCD corrections to jet cross-sections have only been considered for the case of distinguishable quarks[5]. We hope to give a complete discussion of jet cross-sections including all parton subprocesses in a future paper.

The plan of this paper is as follows. In section 2 we calculate all the $(2 \to 2)$ scattering cross-sections in n dimensions including the virtual corrections, giving full details of our method of calculation. In section 3 we present results for all the $(2 \to 3)$ scattering cross-sections in n dimensions. Section 4 discusses one hadron inclusive scattering, which is the theoretically simplest physical application of our results. We make a comparison with previous work on this process and make a preliminary analysis of the corrections to one particle inclusive scattering in a pure gluon theory.

II. The $(2 \to 2)$ Subprocesses.

As a first step in calculation of the higher order corrections we shall consider the effects of virtual radiation on the two-to-two partonic scattering subprocesses. In evaluating these corrections we will encounter ultraviolet, collinear and infra-red divergences, which we regulate by analytic continuation to n space-time dimensions[6]. In this regularisation scheme the divergences appear as poles in the parameter ϵ where $n = 4 - 2\epsilon$. We note in passing that these poles will cancel only when the $(2 \to 2)$ and $(2 \to 3)$ processes are combined to form physical quantities.

The basic processes which we have to consider are,

$$\begin{array}{lll} (a) & q_j + q_k \to q_j + q_k & j \neq k \\ (b) & q_j + q_j \to q_j + q_j & \\ (c) & q_j + \bar{q}_j \to g + g & \\ (d) & g + g \to g + g & \end{array} \tag{2.1}$$

Quarks are everywhere taken to be massless, so our calculations are appropriate for a region far from mass thresholds. We quote the results for these processes in terms of the invariant matrix elements squared and summed over both initial and final colours and spins. In this form the crossing properties,necessary for the derivation of all other $(2 \to 2)$ matrix elements, are manifest. The cross-sections are derived from these squared matrix elements by averaging over the initial colours and spins and including the appropriate phase space factors. The full $2 \to 2$ differential cross-section is then given by,

$$d\sigma = \frac{(2\pi)^{2\epsilon}}{32\pi^2 s} \frac{d^{n-1}p_3}{p_3^0} \frac{d^{n-1}p_4}{p_4^0} \bar{\sum} |M|^2 \, \delta^{(n)}(p_1 + p_2 - p_3 - p_4) \tag{2.2}$$

where $\bar{\sum}$ denotes the averaging over the initial colours and spins, and summing over the final colours and spins. By convention we spin average by dividing by 2 for each quark in the initial state and by $2(1-\epsilon)$ for each gluon in the initial state. Further justification for this choice will be given in Section (IV).

The invariant matrix elements squared for the processes of Eq.(2.1), summed and averaged over colours and spins, define four functions a, b, c, and d as follows,

$$\begin{aligned}
\bar{\sum}\left|M^{q_j q_k \to q_j q_k}\right|^2 &= \frac{1}{4N^2}\left[a(s,t,u)\right] \\
\bar{\sum}\left|M^{q_j q_j \to q_j q_j}\right|^2 &= \frac{1}{4N^2}\left[a(s,t,u) + a(s,u,t) + b(s,t,u)\right] \\
\bar{\sum}\left|M^{q_j \bar{q}_j \to gg}\right|^2 &= \frac{1}{4N^2}\left[c(s,t,u)\right] \\
\bar{\sum}\left|M^{gg \to gg}\right|^2 &= \frac{1}{4(1-\epsilon)^2 V^2}\left[d(s,t,u)\right]
\end{aligned} \tag{2.3}$$

where

$$s = (p_1 + p_2)^2, \qquad t = (p_1 - p_3)^2, \qquad u = (p_2 - p_3)^2 \tag{2.4}$$

The matrix elements squared for all two-to-two processes can be obtained from the functions a, b, c and d as shown in Table 1. Throughout this paper we employ the notation that $N = 3$ is the number of colours and V is the dimensionality of the vector representation of the $SU(N)$ group ($V = N^2 - 1$).

The functions a, b, c and d have perturbative expansions which we write as,

$$\begin{aligned}
a(s,t,u) &\to g^4\,(\mu)^{4\epsilon} a^{(4)}(s,t,u) + g^6\,(\mu)^{6\epsilon} a^{(6)}(s,t,u) + O(g^8) \\
b(s,t,u) &\to g^4\,(\mu)^{4\epsilon} b^{(4)}(s,t,u) + g^6\,(\mu)^{6\epsilon} b^{(6)}(s,t,u) + O(g^8) \\
c(s,t,u) &\to g^4\,(\mu)^{4\epsilon} c^{(4)}(s,t,u) + g^6\,(\mu)^{6\epsilon} c^{(6)}(s,t,u) + O(g^8) \\
d(s,t,u) &\to g^4\,(\mu)^{4\epsilon} d^{(4)}(s,t,u) + g^6\,(\mu)^{6\epsilon} d^{(6)}(s,t,u) + O(g^8)
\end{aligned} \tag{2.5}$$

$a^{(4)}, b^{(4)}, c^{(4)}$ and $d^{(4)}$ have been calculated in 4 dimensions in ref. [7]. Since we are using dimensional regularisation we need the n dimensional forms for these functions. The relevant Feynman diagrams are shown in Fig. 1 and the n dimensional results are presented in Table 2. We note that the n dimensional results for $b^{(4)}$ and $d^{(4)}$ are in disagreement with the results of ref.[8]. All results are in agreement with ref.[7] in the limit $\epsilon \to 0$.

Radiative Corrections to $q_j + q_k \rightarrow q_j + q_k$.

We now turn to the calculation of the first radiative correction to the elastic scattering of distinguishable quarks. The relevant Feynman amplitudes are shown in Fig. 1a and Fig. 2. The correction we seek comes from the the interference of the single tree diagram of Fig. 1a with the five one-loop 'master' diagrams of Fig. 2.

This particular calculation is the simplest of the various matrix elements which we must calculate and the results have already been presented in elsewhere[1,2]. However the number of graphs involved in the calculation of the radiative corrections for all two-to-two processes requires that the problem be reformulated in such a way that it may be efficiently handled by the algebraic manipulation program Schoonschip[9]. We therefore describe the case of quark-quark scattering in some detail as an illustration of our calculational techniques.

Consider first the master diagrams shown in Fig. 2. In this figure solid lines represent quarks, curly lines represent gluons, ghosts, or anti-ghosts and dashed lines represent gluons, ghosts, anti-ghosts, quarks, or anti-quarks. An implicit sum over the various allowed partons is assumed for each type of line. Thus, for example, master diagram 1 of Fig. 2 represents five distinct Feynman diagrams each with the same basic topology. These five diagrams are shown in Fig. 3 and correspond, in turn, to a gluon flowing round the loop, a ghost flowing in either of two directions around the loop, or a quark flowing in either of two directions around the loop. The program generates these five diagrams from the master diagram by allowing every dashed line to run over all five possibilities and eliminating those diagrams which fail to satisfy the conservation of ghost number or of fermion number at every vertex. Once the diagrams have been generated it is straightforward to include the minus sign for any ghost or fermion loops which are present and to insert the Feynman rules for the various vertices and propagators.

Note that the above procedure automatically generates the correct statistical weight for the gluon diagrams relative to the ghost and quark diagrams[10]. The two directions of ghost and quark loops lead to identical expressions and are therefore not normally considered as separate graphs. It follows that a single quark or ghost diagram enters with a weight of two relative to the gluon loop diagram. After multiplying by an overall factor of $\frac{1}{2}$ we get the normal statistical factor for the gluon self-energy. By working through a few examples it can be seen that this method of inclusion of statistical factors works for all diagrams.

The above discussion of the diagrams of Fig. 2 explains the significance of the dashed and curly lines. This notation is used throughout this paper. However the basic quantities which we use to calculate the radiative corrections to parton parton scattering are not the amplitudes themselves but rather the cut graphs generated by the interferences of the Born amplitude with the radiatively corrected amplitude. Interfering the diagram of Fig. 1a with the five master diagrams of Fig. 2 we obtain only four distinct topologies of cut diagrams. These topologies are shown in Fig. 4. The reduction in the number of diagrams as we pass from the amplitudes of Fig. 2 to these cut diagrams occurs because the interferences of diagrams 2 and 3 with the Born term of Fig. 1a generate cut diagrams with exactly the same topology (topology 2 of Fig. 4). This simplification is exploited wherever possible in the following calculations.

At this point we have reduced the problem of calculating the radiative corrections to that of evaluating the four cut topologies shown in Fig. 4. We denote the result of the i^{th} topology by $\Gamma_i^{(a)}(p_1, p_2, p_3, p_4)$. The arguments of the function $\Gamma_i^{(a)}$ are the momenta crossing the cut in Fig. 4 (or equivalently the external momenta in the amplitudes of Figs 1a and 2).

In terms of these topologies the full result for the correction may be written as,

$$\begin{aligned} g^6(\mu)^{6\epsilon} a^{(6)}(s,t,u) = \\ 2\Big\{\frac{1}{2}\,\Gamma_1^{(a)}(p_1,p_2,p_3,p_4) + \Gamma_2^{(a)}(p_1,p_2,p_3,p_4) + \Gamma_2^{(a)}(p_2,p_1,p_4,p_3) \\ + \Gamma_3^{(a)}(p_1,p_2,p_3,p_4) + \Gamma_4^{(a)}(p_1,p_2,p_3,p_4)\Big\} \end{aligned} \tag{2.6}$$

The overall factor of two in this equation comes from the squaring of the amplitude. The factor of $\frac{1}{2}$ which multiplies $\Gamma_1^{(a)}$ is the normal statistical factor associated with the gluon self-energy. Such factors will always be written explicitly. Eq.(2.6) contains in all five terms corresponding to the five distinct interferences.

All five interferences can be obtained from the four cut diagrams by performing the momentum interchanges $(p_1 \leftrightarrow p_2)$ and $(p_3 \leftrightarrow p_4)$. Topologies 1,3 and 4 are unchanged by this permutation. The action of the permutation on Topology 2 is to generate the second interference (see Eq.(2.6)).

To implement this procedure in a more formal way we define a function $F^{(a)}$ which is obtained from the four topologies of Fig. 4 by summing over the results of the topologies Γ_i, weighted with the statistical factors S_i, and multiplied by the weight factor W_i which takes into account the number of interferences obtained from a given topology by permutation of the external momenta.

$$F^{(a)}(p_1,p_2,p_3,p_4) = 2\sum_{i=1,4} S_i^{(a)} W_i^{(a)} \Gamma_i^{(a)}(p_1,p_2,p_3,p_4) \tag{2.7}$$

The statistical and weight factors for distinguishable quark-quark scattering can be read off from Eq.(2.6) or Table 3. The sixth order result for $a^{(6)}$ is finally obtained by appropriate symmetrisation in the external momenta.

$$g^6(\mu)^{6\epsilon} a^{(6)}(s,t,u) = \frac{1}{2}\left[F^{(a)}(p_1,p_2,p_3,p_4) + F^{(a)}(p_2,p_1,p_4,p_3)\right] \tag{2.8}$$

We are now in a position to write down the final result for the matrix element, squared and summed over initial and final spins and colours, up to and including $O(g^6)$. We find,

$$\begin{aligned}
&a(s,t,u) = \\
&g^4(\mu^2)(\mu)^{4\epsilon} a^{(4)}(s,t,u)\Bigg\{1 + \frac{\alpha_S}{2\pi}\left(\frac{4\pi\mu^2}{Q^2}\right)^{\epsilon} \frac{\Gamma(1+\epsilon)\Gamma^2(1-\epsilon)}{\Gamma(1-2\epsilon)} \\
&\Bigg[\frac{V}{2N}\left(-\frac{4}{\epsilon^2} - \frac{1}{\epsilon}\left(6 + 8l(s) - 8l(u) - 4l(t)\right)\right) + \frac{N}{\epsilon}\left(4l(s) - 2l(u) - 2l(t)\right) \\
&+\frac{V}{2N}\Big(-16 - 2l^2(t) + l(t)\left(6 + 8l(s) - 8l(u)\right) \\
&-2\left(\frac{s^2-u^2}{s^2+u^2}\right)\left(2\pi^2 + (l(t)-l(s))^2 + (l(t)-l(u))^2\right) \\
&+2\left(\frac{s+u}{s^2+u^2}\right)\left((s+u)(l(u)-l(s)) + (u-s)(2l(t)-l(s)-l(u))\right)\Big) \\
&+N\Big(\frac{85}{9} + \pi^2 + 2l(t)\left(l(t)+l(u)-2l(s)\right) \\
&+\frac{s^2-u^2}{2(s^2+u^2)}\left(3\pi^2 + 2(l(t)-l(s))^2 + (l(t)-l(u))^2\right) \\
&-\frac{st}{s^2+u^2}\left(l(t)-l(u)\right) + \frac{2ut}{s^2+u^2}\left(l(t)-l(s)\right) + \frac{11}{3}\left(l(-\mu^2)-l(t)\right)\Big) \\
&+T_R\left(\frac{4}{3}\left(l(t)-l(-\mu^2)\right) - \frac{20}{9}\right)\Bigg]\Bigg\} + O(\epsilon)
\end{aligned} \tag{2.9}$$

Eq.(2.9) introduces several new notations which we now define. The colour structure is fixed in terms of the quantities,

$$V = N^2 - 1, \qquad N = 3, \qquad T_R = \frac{n_f}{2}$$

and $g(\mu^2)$ is the coupling constant renormalised at scale μ^2 in the $\overline{MS}$ scheme[11]. n_f is the number of quark flavours. The running coupling constant $\alpha_S = g^2/4\pi$ satisfies the equation,

$$\mu^2 \frac{d}{d\mu^2}\alpha_S = -\alpha_S \left[b_0 \left(\frac{\alpha_S}{2\pi}\right) + b_1 \left(\frac{\alpha_S}{2\pi}\right)^2 + O(\alpha_S{}^3) \right] \tag{2.10}$$

where[12,13],

$$b_0 = \frac{11N}{6} - \frac{2T_R}{3}, \qquad b_1 = \frac{17N^2}{6} - \frac{5NT_R}{3} - \frac{VT_R}{2N} \tag{2.11}$$

The asymptotic behaviour can hence be written as,

$$\frac{\alpha_S(\mu^2)}{2\pi} = \frac{1}{b_0 \ln\left(\frac{\mu^2}{\Lambda^2}\right)} \left[1 - \frac{b_1}{b_0^2} \frac{\ln\ln\left(\frac{\mu^2}{\Lambda^2}\right)}{\ln\left(\frac{\mu^2}{\Lambda^2}\right)} + O\left(\frac{1}{\ln^2\left(\frac{\mu^2}{\Lambda^2}\right)} \right) \right] \tag{2.12}$$

In fixed order perturbation theory the coupling constant has the perturbative expansion,

$$g^4(\mu^2) = g^4(Q^2)\left(1 - 2b_0 \frac{\alpha_S}{2\pi} \ln\left(\frac{\mu^2}{Q^2}\right) + O(\alpha_S{}^2)\right) \tag{2.13}$$

Finally, the notation $l(x)$ denotes the logarithm,

$$l(x) = \ln\left(-\frac{x}{Q^2}\right)$$

If x is greater than zero $l(x)$ has an imaginary part since $Q^2 > 0$. In Eq.(2.9) and following equations it is understood that only the real part is kept. Explicitly we write,

$$\begin{aligned}
l^2(x) &\to \ln^2\left(\frac{x}{Q^2}\right) - \pi^2 \qquad x > 0 \\
l^2(x) &\to \ln^2\left(-\frac{x}{Q^2}\right) \qquad x < 0 \\
l(x) &\to \ln\left(\left|\frac{x}{Q^2}\right|\right)
\end{aligned} \tag{2.14}$$

These assignments should be made after crossing to the appropriate region. Q^2 is an arbitrary momentum scale. It will often be most convenient to make the choice $Q^2 = s$ but we have left it arbitrary to make the behaviour under crossing manifest. We note that the result presented here is in agreement with the results of refs. [1, 2].

Radiative Corrections to $q_j q_j \to q_j q_j$.

If the scattered quarks are identical, there are ten interferences between the diagrams of Fig. 1b and Fig. 2. which generate new topologies not included in Fig. 4. These additional topologies of cut diagrams are shown in Fig. 5. The statistical factors and weights for these diagrams are given in Table 4. All of the interferences are generated by making the weighted sum over the topologies of Fig. 5.

$$F^{(b)}(p_1, p_2, p_3, p_4) = 2 \sum_{i=1,4} S_i^{(b)} W_i^{(b)} \Gamma_i^{(b)}(p_1, p_2, p_3, p_4) \tag{2.15}$$

As before the final answer for identical quark-quark scattering is obtained by symmetrising in the external momenta to recover all the diagrams.

$$\begin{aligned} g^6(\mu)^{6\epsilon} b^{(6)}(s,t,u) =& \frac{1}{4}\Big[F^{(b)}(p_1, p_2, p_3, p_4) + F^{(b)}(p_2, p_1, p_3, p_4) \\ &+ F^{(b)}(p_1, p_2, p_4, p_3) + F^{(b)}(p_2, p_1, p_4, p_3)\Big] \end{aligned} \tag{2.16}$$

The result for the additional contribution to identical quark scattering matrix element is,

$$
\begin{aligned}
b(s,t,u) &= g^4(\mu^2)(\mu)^{4\epsilon} b^{(4)}(s,t,u)\Big\{1+\frac{\alpha_S}{2\pi}\left(\frac{4\pi\mu^2}{Q^2}\right)^{\epsilon}\frac{\Gamma(1+\epsilon)\Gamma^2(1-\epsilon)}{\Gamma(1-2\epsilon)} \\
&\left(\frac{V}{2N}\left[-\frac{4}{\epsilon^2}-\frac{1}{\epsilon}\left(6+4l(s)-4l(t)-4l(u)\right)\right.\right. \\
&\left.-16-\frac{3}{2}(l(t)+l(u))^2+2l(s)(l(t)+l(u))+2(l(t)+l(u))-\frac{1}{2}\pi^2\right] \\
&+N\left[\frac{2}{\epsilon}\left(2l(s)-l(t)-l(u)\right)+\frac{85}{9}+\frac{5}{4}(l(t)+l(u))^2\right. \\
&\left.-l(t)l(u)-2l(s)(l(t)+l(u))-\frac{4}{3}(l(t)+l(u))+\frac{5}{4}\pi^2+\frac{11}{3}l(-\mu^2)\right] \\
&+T_R\left[-\frac{20}{9}+\frac{2}{3}\left(l(t)+l(u)-2l(-\mu^2)\right)\right] \\
&\left.\left.+\frac{1}{N}\left[\left(\pi^2+(l(t)-l(u))^2\right)\frac{ut}{2s^2}+\frac{u}{s}l(t)+\frac{t}{s}l(u)\right]\right)\right\}+O(\epsilon)
\end{aligned} \tag{2.17}
$$

Radiative Corrections to $q_j \bar{q}_j \to g + g$.

The three diagrams of Fig. 1c interfered with the radiatively corrected diagrams of Fig. 6 lead to 42 interference terms. These interferences are fully described by the 21 topologies shown in Fig. 7. It is in this sector of the calculation that the power of our method asserts itself, since it automatically deals with the problem of summing over gluon polarisations in a non-abelian theory. The non-conservation of the gluon current in QCD means that one cannot simply replace the sum over polarisations by,

$$\sum_{polarisations} \epsilon_\mu(p)\epsilon^*_\nu(p) = -g_{\mu\nu} \tag{2.18}$$

If we wish to use Eq. (2.18) to sum over polarisations we must also include ghost contributions (even on external lines) to cancel the unwanted longitudinal polarisations. This is automatically taken care of in Fig. 7, since the curly lines represent either gluons or ghosts/anti-ghosts (if the latter possibility is allowed by ghost number conservation). Thus several diagrams are compactly represented in terms of one topology. The weighted (but unsymettrised) sum over topologies is given by,

$$F^{(c)}(p_1,p_2,p_3,p_4) = 2\sum_{i=1,21} S_i^{(c)} W_i^{(c)} \Gamma_i^{(c)}(p_1,p_2,p_3,p_4) \tag{2.19}$$

where $S_i^{(c)}$ and $W_i^{(c)}$ are given in Table 7. The final answer for quark anti-quark annihilation is obtained by symmetrisation over external momenta in order to recover all the diagrams,

$$g^6(\mu)^{6\epsilon} c^{(6)}(s,t,u) = \frac{1}{2}\left[F^{(c)}(p_1,p_2,p_3,p_4) + F^{(c)}(p_1,p_2,p_4,p_3)\right] \tag{2.20}$$

The result is,

$$
\begin{aligned}
c(s,t,u) &= g^4(\mu^2)(\mu)^{4\epsilon}\Big\{ c^{(4)}(s,t,u)\Big(1+\frac{\alpha_S}{2\pi}\left(\frac{4\pi\mu^2}{Q^2}\right)^{\epsilon}\frac{\Gamma(1+\epsilon)\Gamma^2(1-\epsilon)}{\Gamma(1-2\epsilon)} \\
&\left[\frac{V}{2N}\left(-\frac{2}{\epsilon^2}-\frac{3}{\epsilon}-7\right)+N\left(-\frac{2}{\epsilon^2}-\frac{11}{3\epsilon}+\frac{11}{3}l(-\mu^2)\right)+T_R\left(\frac{4}{3\epsilon}-\frac{4}{3}l(-\mu^2)\right)\right]\Big) \\
&+\frac{\alpha_S}{2\pi}\left(\frac{4\pi\mu^2}{Q^2}\right)^{\epsilon}\frac{\Gamma(1+\epsilon)\Gamma^2(1-\epsilon)}{\Gamma(1-2\epsilon)} \\
&\left[\frac{l(s)}{\epsilon}\left(\left((2N^2V+\frac{2V}{N^2}\right)\frac{t^2+u^2}{ut}-4V^2\frac{t^2+u^2}{s^2}\right)\right. \\
&+\frac{4N^2V}{\epsilon}\left(l(t)\left(\frac{u}{t}-\frac{2u^2}{s^2}\right)+l(u)\left(\frac{t}{u}-\frac{2t^2}{s^2}\right)\right) \\
&\left.-\frac{4V}{\epsilon}\left(\frac{u}{t}+\frac{t}{u}\right)(l(t)+l(u))\right] \\
&+\frac{\alpha_S}{2\pi}\left(f^c(s,t,u)+f^c(s,u,t)\right)\Big\}+O(\epsilon)
\end{aligned}
\tag{2.21}
$$

where f^c is given by

$$
\begin{aligned}
f^c(s,t,u) &= 4NV\left\{\frac{l(t)l(u)}{N}\left(\frac{t^2+u^2}{2tu}\right)\right. \\
&+l^2(s)\left(\frac{1}{4N^3}\frac{s^2}{tu}+\frac{1}{4N}\left(\frac{1}{2}+\frac{t^2+u^2}{tu}-\frac{t^2+u^2}{s^2}\right)-\frac{N}{4}\left(\frac{t^2+u^2}{s^2}\right)\right) \\
&+l(s)\left(\left(\frac{5}{8}\frac{V}{N}-\frac{1}{2N}-\frac{1}{N^3}\right)-\left(N+\frac{1}{N^3}\right)\left(\frac{t^2+u^2}{2tu}\right)-\frac{V}{4N}\left(\frac{t^2+u^2}{s^2}\right)\right) \\
&+\pi^2\left(\frac{1}{8N}+\frac{1}{N^3}\left(\frac{3(t^2+u^2)}{8tu}+\frac{1}{2}\right)+N\left(\frac{t^2+u^2}{8tu}-\frac{t^2+u^2}{2s^2}\right)\right) \\
&+\left(N+\frac{1}{N}\right)\left(\frac{1}{8}-\frac{t^2+u^2}{4s^2}\right) \\
&+l^2(t)\left(N\left(\frac{s}{4t}-\frac{u}{s}-\frac{1}{4}\right)+\frac{1}{N}\left(\frac{t}{2u}-\frac{u}{4s}\right)+\frac{1}{N^3}\left(\frac{u}{4t}-\frac{s}{2u}\right)\right) \\
&+l(t)\left(N\left(\frac{t^2+u^2}{s^2}+\frac{3t}{4s}-\frac{5u}{4t}-\frac{1}{4}\right)-\frac{1}{N}\left(\frac{u}{4s}+\frac{2s}{u}+\frac{s}{2t}\right)-\frac{1}{N^3}\left(\frac{3s}{4t}+\frac{1}{4}\right)\right) \\
&\left.+l(s)l(t)\left(N\left(\frac{t^2+u^2}{s^2}-\frac{u}{2t}\right)+\frac{1}{N}\left(\frac{u}{2s}-\frac{t}{u}\right)+\frac{1}{N^3}\left(\frac{s}{u}-\frac{u}{2t}\right)\right)\right\}
\end{aligned}
\tag{2.22}
$$

Radiative Corrections to $g + g \to g + g$.

The four diagrams of Fig. 1d interfered with the radiative correction diagrams of Fig. 8 (including the diagrams obtained by interchange of the legs) yield 108 combinations. These interferences can all be obtained from the 18 topologies shown in Fig. 8. Here again the curly line represents gluons or ghosts/anti-ghosts. Thus a single topology in Fig. 8 may represent many diagrams corresponding to the different ways of looping gluons, ghosts or fermions through the diagram. The weighted sum over topologies is

$$F^{(d)}(p_1, p_2, p_3, p_4) = 2 \sum_{i=1,18} S_i^{(d)} W_i^{(d)} \Gamma_i^{(d)}(p_1, p_2, p_3, p_4) \tag{2.23}$$

where the weights and statistical factor are given in Table 6. The final answer is given by the permutation over all momenta to generate all the interferences.

$$g^6(\mu)^{6\epsilon} d^{(6)}(s,t,u) = \frac{1}{4!} \sum_{permutations} \left[F^{(d)}(p_1, p_2, p_3, p_4)\right] \tag{2.24}$$

We find,

$$\begin{aligned}
d(s,t,u) = {} & g^4(\mu^2)(\mu)^{4\epsilon}\Bigg\{ d^{(4)}(s,t,u) \\
& + \frac{\alpha_S}{2\pi}\left(\frac{4\pi\mu^2}{Q^2}\right)^{\epsilon} \frac{\Gamma(1+\epsilon)\Gamma^2(1-\epsilon)}{\Gamma(1-2\epsilon)} \Bigg[d^{(4)}(s,t,u) \\
& \left(-\frac{4N}{\epsilon^2} - \frac{22N}{3\epsilon} + \frac{8T_R}{3\epsilon} - \frac{67N}{9} + \frac{20T_R}{9} + N\pi^2 + \frac{11N}{3} l(-\mu^2) - \frac{4T_R}{3} l(-\mu^2)\right) \\
& + \frac{16VN^3}{\epsilon} l(s) \left(3 - \frac{2tu}{s^2} + \frac{(t^4+u^4)}{t^2u^2}\right) \\
& + \frac{16VN^3}{\epsilon} l(t) \left(3 - \frac{2us}{t^2} + \frac{(u^4+s^4)}{u^2s^2}\right) \\
& + \frac{16VN^3}{\epsilon} l(u) \left(3 - \frac{2st}{u^2} + \frac{(s^4+t^4)}{s^2t^2}\right) \Bigg] \\
& + \frac{\alpha_S}{2\pi} 4VN^2 \left(f^d(s,t,u) + f^d(t,u,s) + f^d(u,s,t)\right) \Bigg\} + O(\epsilon)
\end{aligned} \tag{2.25}$$

where f^d is given by,

$$
\begin{aligned}
f^d(s,t,u) = N \Bigg[& \left(\frac{2(t^2+u^2)}{tu}\right) l^2(s) + \left(\frac{4s(t^3+u^3)}{t^2u^2} - 6\right) l(t)l(u) \\
& + \left(\frac{4}{3}\frac{tu}{s^2} - \frac{14}{3}\frac{(t^2+u^2)}{tu} - 14 - 8\left(\frac{t^2}{u^2}+\frac{u^2}{t^2}\right)\right) l(s) - 1 - \pi^2 \Bigg] \\
& + T_R \Bigg[\left(\frac{10}{3}\frac{(t^2+u^2)}{tu} + \frac{16}{3}\frac{tu}{s^2} - 2\right) l(s) - \left(\frac{s^2+tu}{tu}\right) l^2(s) \\
& - 2\left(\frac{t^2+u^2}{tu}\right) l(t)l(u) + 2 - \pi^2 \Bigg]
\end{aligned}
\tag{2.26}
$$

Finally we note that the poles present in Eqs.(2.9,2.17,2.21,2.25) are a consequence of the singularities due to the emission of soft and collinear radiation. Also note that as expected the terms containing the soft singularity have the same kinematic structure as the lowest order matrix element.

III. The $2 \to 3$ parton subprocesses.

In order to regulate the singularities which are present due to soft or collinear emission of partons, we need the matrix element squared for the $2 \to 3$ parton processes in n dimensions. In four dimensions, these subprocesses were first calculated by Gottschalk and Sivers and by Kunszt and Pietarinen[14]. More recently, extremely compact and elegant forms for the four dimensional results for these processes have been given by Berends et al[15]. In our calculation we followed closely the procedure of ref.[14], (which is extremely similar to the method used for the virtual diagrams described in the previous section). We have checked that our formula reduce to the formula of ref.[15] in the limit $n \to 4$. Although we are in agreement with their basic approach, we have not checked the long answer in the first of refs.[14] in every detail.

We calculate the amplitudes for the processes,

$$\begin{array}{lll} (A) & q_j + q_k \to q_j + q_k + g & j \neq k \\ (B) & q_j + q_j \to q_j + q_j + g & \\ (C) & q_j + \bar{q}_j \to g + g + g & \\ (D) & g + g \to g + g + g & \end{array} \tag{3.1}$$

We present results for the matrix elements squared for these four basic processes summed over colours and spins (but, as before, without averaging over initial colours or spins). We calculate these amplitudes in an unphysical configuration in which all momenta are incoming,

$$p_1 + p_2 + p_3 + p_4 + p_5 = 0 \tag{3.2}$$

All other amplitudes are obtained from those of Eq.(3.1) by crossing as detailed in Table.7.

We define the following notation to assist in writing down a compact form for the answers,

$$V_1 = \frac{(N^2-1)^2}{N}, \qquad V_2 = \frac{(N^2-1)}{N}, \qquad V_3 = \frac{N^4-1}{2N^2}, \qquad V_4 = \frac{(N^2-1)^2}{2N^2}.$$

In addition we define the variables

$$
\begin{array}{lll}
s = 2p_1.p_2, & s' = 2p_3.p_4, & s_\pm = (s \pm s')/2 \\
t = 2p_1.p_3, & t' = 2p_2.p_4, & t_\pm = (t \pm t')/2 \\
u = 2p_1.p_4, & u' = 2p_2.p_3, & u_\pm = (u \pm u')/2
\end{array}
\tag{3.3}
$$

The definition of t, t', u and u' given in Eq.(3.3) is the one appropriate for the configuration in which all momenta are incoming. After continuation to the physical region of process A, these definitions of s, t and u coincide with the normal definitions given in Eq.(2.4). The result for process A in the unphysical region (Eq.(3.2)) is,

$$
\begin{aligned}
&A(p_1,p_2,p_3,p_4,p_5) = \\
&g^6(\mu)^{6\epsilon}\{V_1(s_+^2 + s_-^2 + u_+^2 + u_-^2) \\
&[0.5u_+(ss' + tt' - uu') + 0.25u(st + s't') + 0.25u'(st' + s't)] \\
&- V_2(s_+^2 + s_-^2 + u_+^2 + u_-^2)[0.5s_+(ss' - tt' - uu') + u_+tt' + t_+uu'] \\
&+ \epsilon V_1[(u_+(s_-^2 + u_-^2 + 0.5t_+^2) + 0.25t_+(1-2\epsilon)(s_-^2 - t_-^2 - u_-^2))(s_-^2 + t_-^2 - u_-^2) \\
&- s_-t_-u_-(2s_-^2 + 2u_-^2 + t_+^2) - t_-^3 s_-u_-(1-2\epsilon)] \\
&+ \epsilon V_2[-0.5t_+^2(s_+(s_-^2 - t_-^2 - u_-^2) + 2u_+t_-^2 + 2t_+u_-^2) \\
&+ 0.25t_+(1-2\epsilon)(s_-^4 + t_-^4 + u_-^4 - 2s_-^2t_-^2 - 2s_-^2u_-^2 - 2t_-^2u_-^2) \\
&- s_+(s_-^4 - u_-^4) - 2t_+u_-^4 + (s_+ - 2u_+)t_-^2(s_-^2 + u_-^2) - 2t_+s_-^2u_-^2]\} \\
&/t/t'/p_1.p_5/p_2.p_5/p_3.p_5/p_4.p_5
\end{aligned}
\tag{3.4}
$$

The matrix elements squared for the physical processes can be obtained from the function A as shown in Table.7.

The corresponding result for the case of identical quarks (process B) is given by,

$$
\begin{aligned}
&B(p_1,p_2,p_3,p_4,p_5) = A(p_1,p_2,p_3,p_4,p_5) + A(p_1,p_2,p_4,p_3,p_5)\\
&+g^6(\mu)^{6\epsilon}\{(ss'-tt'-uu')(s^2+s'^2)V_3\\
&\quad[0.25s_+(ss'-tt'-uu')+0.5u_+tt'+0.5t_+uu']\\
&+(ss'-tt'-uu')(s^2+s'^2)V_4\\
&\quad[0.25s_+(ss'-tt'-uu')-0.5u_+tt'-0.5t_+uu'-0.25s(tu+t'u')-0.25s'(tu'+ut')]\\
&-\epsilon(ss'-tt'-uu')\\
&\quad[-0.25(5+\epsilon)(V_3+V_4)s_+(s_-^2-t_-^2-u_-^2)^2\\
&\quad+\{(0.5(1+\epsilon)(1-2\epsilon)(V_3+V_4)-0.5(5+\epsilon)(V_3-V_4))(t_-^2u_++u_-^2t_+)\\
&\quad-(1-\epsilon)(V_3+V_4)s_+(t_-^2+u_-^2)-0.5(V_3+V_4)s_+(t_+^2+u_+^2+t_-^2+u_-^2)\\
&\quad-(5+\epsilon)V_4s_-t_-u_-\}(s_-^2-t_-^2-u_-^2)\\
&\quad-2V_4s_-t_-u_-\{(t_+^2+u_+^2+t_-^2+u_-^2)\\
&\quad+2(1-\epsilon)(t_-^2+u_-^2)+(1+\epsilon)(1-2\epsilon)t_+u_+\}\\
&\quad+(1+\epsilon)(V_3+V_4)s_+tt'uu'\\
&\quad-(V_3-V_4)(t_-^2u_++u_-^2t_+)(t_+^2+u_+^2+t_-^2+u_-^2)\\
&\quad-2(1-\epsilon)(V_3-V_4)(t_-^2u_++u_-^2t_+)(t_-^2+u_-^2)+(1+\epsilon)(1-2\epsilon)(V_3-V_4)s_+t_-^2u_-^2]\\
&+\epsilon(1+\epsilon)tt'uu'\\
&\quad[2V_3(s_+t_+u_++t_+u_-^2+u_+t_-^2)+2V_4(s_+t_+u_+-t_+u_-^2-u_+t_-^2)+8\epsilon V_4s_-t_-u_-]\}\\
&\quad/p_1{\cdot}p_5/p_2{\cdot}p_5/p_3{\cdot}p_5/p_4{\cdot}p_5/t/t'/u/u'
\end{aligned}
\tag{3.5}
$$

The result for the process C is symmetric under the interchange of the three gluons and under the interchange of the quark and anti-quark. It can therefore be written as the sum of 12 permutations corresponding to these symmetries.

$$
C(p_1,p_2,p_3,p_4,p_5) = g^6(\mu)^{6\epsilon} \sum_{12\ permutations} F^C(1,2,3,4,5) \tag{3.6}
$$

where F^C is given by,

$$
\begin{aligned}
&F^C(1,2,3,4,5) = \frac{V}{N^2}\Big\{-N^2(1-\epsilon)^2(a_+b_+ - a_-b_-)/p_3{\cdot}p_4 \\
&\quad [2(a_+^2 + a_-^2)/p_1{\cdot}p_4/p_2{\cdot}p_4/p_1{\cdot}p_5/p_2{\cdot}p_5 + (c_+^2 + c_-^2)/p_1{\cdot}p_3/p_2{\cdot}p_3/p_1{\cdot}p_4/p_2{\cdot}p_4] \\
&+N^4(1-\epsilon)(a_+b_+ - a_-b_-)/p_1{\cdot}p_2/p_4{\cdot}p_5/p_3{\cdot}p_5 \\
&\quad [2(b_+^2 + b_-^2)/p_1{\cdot}p_3/p_2{\cdot}p_3 + (c_+^4 - c_-^4)/p_1{\cdot}p_4/p_2{\cdot}p_4/p_1{\cdot}p_3/p_2{\cdot}p_3] \\
&+(N^2+1)0.25p_1{\cdot}p_2[2(1-\epsilon)^2(c_+^2 + c_-^2) - \delta_1(a_+^2 + a_-^2 + b_+^2 + b_-^2 - c_+^2 - c_-^2) \\
&\quad - 2\delta_2(c_+^2 - c_-^2) - \delta_3(a_+^2 - a_-^2 + b_+^2 - b_-^2 - c_+^2 + c_-^2)]/p_1{\cdot}p_3/p_2{\cdot}p_3/p_1{\cdot}p_4/p_2{\cdot}p_4 \\
&+N^2(-\epsilon(1+3\epsilon)(a_+^2 - a_-^2 + b_+^2 - b_-^2) \\
&\quad (p_1{\cdot}p_3p_1{\cdot}p_4p_1{\cdot}p_5 - p_2{\cdot}p_3p_2{\cdot}p_4p_2{\cdot}p_5)0.5c_-)/p_3{\cdot}p_4/p_1{\cdot}p_3/p_2{\cdot}p_3/p_1{\cdot}p_4/p_2{\cdot}p_4/p_1{\cdot}p_5/p_2{\cdot}p_5 \\
&+2N^2\delta_2(a_+b_+ - a_-b_-)/p_1{\cdot}p_5/p_2{\cdot}p_5/p_3{\cdot}p_4 \\
&+N^2\{0.5(\delta_1 - 2\delta_2 + \delta_3)(a_+ + b_+ - c_+)(a_+ + b_+ + c_+) \\
&\quad ((a_+ + b_+)(a_+ + b_+ - c_+) - a_+b_+ - 3a_-b_-) + 2\delta_2a_+b_+(a_+^2 + b_+^2) \\
&\quad + (2\delta_3 - 6\delta_2)a_-b_-(a_+^2 + b_+^2) + (\delta_3 - 4\delta_2)a_+b_+c_-^2 \\
&\quad + \delta_3a_-b_-(a_-^2 + b_-^2) + (2\delta_2 - \delta_3)c_+(a_+b_-^2 + a_-^2b_+) \\
&\quad + (6\delta_2 - 3\delta_3)a_-b_-(a_+ + b_+)c_+ + (6\delta_3 - 8\delta_2)a_+b_+a_-b_-\}/p_3{\cdot}p_4/p_1{\cdot}p_3/p_2{\cdot}p_3/p_1{\cdot}p_4/p_2{\cdot}p_4 \\
&+N^4\{-2\delta_2(a_+b_+ - a_-b_-)c_+^4 - \delta_2(a_+ + b_+)^3c_+a_+b_+ \\
&\quad + 2\delta_2(a_+b_+ - a_-b_-)c_+^2c_-^2 + \delta_2(a_+b_+ + a_-b_-)(a_+ + b_+)c_+^3 \\
&\quad + \delta_2(a_+b_- + a_-b_+)c_+^3c_- - \delta_2a_+b_+(a_+^2 - a_-^2 + b_+^2 - b_-^2)c_+^2 \\
&\quad + 4\delta_2(a_+^2 - a_-^2)(b_+^2 - b_-^2)c_+^2 + 2\delta_2(a_+b_+ + a_-b_-)(a_+b_+ - a_-b_-)c_+^2 \\
&\quad + \delta_2c_+(a_+ + b_+)(a_+b_+ - a_-b_-)^2 \\
&\quad - 2\delta_2(a_+b_+ - a_-b_-)(a_+b_- + a_-b_+)c_+c_- - \delta_2(a_+b_+ + a_-b_-)(a_+ + b_+)c_+a_-b_- \\
&\quad - \delta_2(a_+b_- + a_-b_+)a_+b_+c_+c_- + \delta_2a_+b_+(a_+ + b_+)c_+c_-^2 \\
&\quad - 2\delta_2(a_+^2 - a_-^2 + b_+^2 - b_-^2)a_+b_+a_-b_- + 2\delta_2(a_+b_+ - a_-b_-)(a_+^2 + b_+^2)(a_-^2 + b_-^2) \\
&\quad - 2\delta_2(a_+b_+ - a_-b_-)(a_+^2 + b_+^2)^2 + \delta_2a_+^4(b_+^2 - b_-^2) \\
&\quad + \delta_2b_+^4(a_+^2 - a_-^2) + \delta_2a_+b_+a_+^2(a_+^2 - a_-^2) + \delta_2a_+b_+b_+^2(b_+^2 - b_-^2) \\
&\quad + 0.5(\delta_1 + \delta_3)(a_+b_+ - a_-b_-)[a_+^4 + b_+^4 + c_+^4 - 2a_+^2b_+^2 - 2a_+^2c_+^2 - 2b_+^2c_+^2] \\
&\quad - \delta_3(a_+b_+ - a_-b_-)[a_+^2a_-^2 + b_+^2b_-^2 + c_+^2c_-^2] \\
&\quad + \delta_3(a_+b_+ - a_-b_-)[a_+^2b_-^2 + a_-^2b_+^2 + a_+^2c_-^2 + a_-^2c_+^2 + b_+^2c_-^2 + b_-^2c_+^2]\} \\
&\quad /p_1{\cdot}p_2/p_3{\cdot}p_5/p_4{\cdot}p_5/p_1{\cdot}p_3/p_2{\cdot}p_3/p_1{\cdot}p_4/p_2{\cdot}p_4\Big\}
\end{aligned}
\tag{3.7}
$$

To simplify the formula we have defined,

$$\delta_1 = \epsilon(1-\epsilon)^2, \qquad \delta_2 = \epsilon(1-\epsilon), \qquad \delta_3 = \epsilon(3+\epsilon), \tag{3.8}$$

and,

$$\begin{aligned} a_+ &= (p_1.p_3 + p_2.p_3)/2, & a_- &= (p_1.p_3 - p_2.p_3)/2, \\ b_+ &= (p_1.p_4 + p_2.p_4)/2, & b_- &= (p_1.p_4 - p_2.p_4)/2, \\ c_+ &= (p_1.p_5 + p_2.p_5)/2, & c_- &= (p_1.p_5 - p_2.p_5)/2, \end{aligned} \tag{3.9}$$

The quantities δ_1, δ_2 and δ_3 vanish in the limit $n \to 4$. In this limit it is only the first six lines of Eq.(3.7) which contribute to C in agreement with the results of ref.[15].

The result for the base function D which describes the five gluon transition probability is most conveniently written by introducing the compact notation for the dot-product

$$p_i.p_j = (ij) \tag{3.10}$$

The function D is a completely symmetric function of the momenta of the five gluons. It can be expressed as the sum over all 5 factorial permutations of the arguments of the function F^D,

$$D(p_1,p_2,p_3,p_4,p_5) = g^6(\mu)^{6\epsilon}\,\frac{1}{10}\sum_{permutations} F^D(1,2,3,4,5) \tag{3.11}$$

where

$$\begin{aligned} F^D(1,2,3,4,5) = &\frac{4VN^3}{(12)(23)(34)(45)(51)} \\ &\Big[\frac{(1-\epsilon)^2}{2}\Big\{(12)^4 + (13)^4 + (14)^4 + (15)^4 + (23)^4 \\ &\qquad + (24)^4 + (25)^4 + (34)^4 + (35)^4 + (45)^4\Big\} \\ &- 3\delta_3\Big\{(12)^2(23)^2 + (23)^2(34)^2 + (34)^2(45)^2 + (45)^2(51)^2 + (51)^2(12)^2\Big\} \\ &+ 6\delta_3\Big\{(12)(23)^2(34) + (23)(34)^2(45) + (34)(45)^2(51) \\ &\qquad + (45)(51)^2(12) + (51)(12)^2(23)\Big\} \\ &- 6\delta_3\{(12)(23)(34)(45) + (23)(34)(45)(51) + (34)(45)(51)(12) \\ &\qquad + (45)(51)(12)(23) + (51)(12)(23)(34)\}\Big] \end{aligned} \tag{3.12}$$

Because of the great symmetry we have obtained an extremely compact form for this matrix element squared even in n dimensions. Notice that the last three terms are proportional to δ_3 which vanishes in both four and ten dimensions. We find that the results for the matrix element squared D in four and ten dimensions are proportional. We have no explanation for this simplicity.

IV. One particle inclusive cross-sections.

In this section we apply our results to the calculation of physical cross-sections. The particular process we choose to study is one particle inclusive hadron scattering. From a theoretical standpoint this is the simplest physical quantity which we can calculate. It also allows us to make contact with earlier work and provides a partial check of our results. As a further motivation we note that in ref.[5] the inclusive parton cross-section was used as a preliminary step in the calculation of jet cross-sections.

In QCD the inclusive cross-section for the production of a hadron H_3 at large transverse momentum P_T,

$$H_1(P_1) + H_2(P_2) \to H_3(P_3) + X \tag{4.1}$$

may be written in the factorised form,

$$\begin{aligned} E_3\frac{d^3\sigma^H}{d^3P_3} = \sum_{i,j,k}\int_0^1 dx_1 dx_2 \frac{dx_3}{x_3^2} \\ \left[D_k^{H_3}(x_3,\mu^2)\left\{\hat{p}_3^0\frac{d^3\hat{\sigma}_{ij}^k(\alpha_S(\mu^2))}{d^3\hat{p}_3}\right\}F_j^{H_2}(x_2,\mu^2)F_i^{H_1}(x_1,\mu^2)\right] \end{aligned} \tag{4.2}$$

The sum on i,j,k runs over all species of partons. The short distance cross-section $\hat{\sigma}$ is evaluated at re-scaled values of the hadronic momenta,

$$\hat{p}_1 = x_1 P_1, \qquad \hat{p}_2 = x_2 P_2, \qquad \hat{p}_3 = P_3/x_3.$$

$\hat{\sigma}$ is calculable as a perturbation series in the running coupling constant $\alpha_S(\mu^2)$. F and D are the non-perturbative distribution and decay functions. These functions must be determined from experiment but their dependence of the scale μ is given by the evolution equations.

$$\begin{aligned} \mu^2\frac{d}{d\mu^2}F_i^H(x,\mu^2) &= \frac{\alpha_S(\mu^2)}{2\pi}\sum_j\int dz dy\, P_{ij}^{(S)}(z)F_j^H(y,\mu^2)\delta(x-yz) \\ \mu^2\frac{d}{d\mu^2}D_i^H(x,\mu^2) &= \frac{\alpha_S(\mu^2)}{2\pi}\sum_j\int dz dy\, D_j^H(y,\mu^2)P_{ji}^{(T)}(z)\delta(x-yz) \end{aligned} \tag{4.3}$$

In these equations $P^{(S,T)}$ are the space-like and time-like evolution probabilities.

They have perturbative expansions, the first two terms of which are given in refs.[16] and [17 – 19] respectively.

The quantity of particular interest to us is the short distance cross-section $\hat{\sigma}$. To calculate $\hat{\sigma}$ we need first to calculate the full one parton inclusive cross-section σ. At order $\alpha_S{}^3$ the cross-section σ has two contributions : the first from the radiatively corrected $(2 \to 2)$ parton processes calculated in Section (II) and the second from the tree level $(2 \to 3)$ parton processes calculated in Section (III). σ is calculated from these results by adding the appropriate phase space factors in n dimensions and integrating over the unobserved degrees of freedom. For details of this procedure we refer the reader to the discussion of ref.[1].

When the contributions of the $(2 \to 2)$ and $(2 \to 3)$ scattering processes are combined to form σ only the soft singularities present in the individual terms cancel. However the factorisation theorem[20,21] assures us that all the remaining singularities may be factored into process-independent functions Γ associated with the incoming and outgoing parton legs. Thus, for the one parton inclusive cross-section in n dimensions, we may write,

$$p_3^0 \frac{d^{n-1}\sigma_{ij}^k}{d^{n-1}p_3} = \sum_{i',j',k'} \int_0^1 dz_1 dz_2 \frac{dz_3}{z_3^2} \left[\Gamma_{kk'}^{(T)}(z_3,\epsilon) \left\{\hat{p}_3^0 \frac{d^{n-1}\hat{\sigma}_{i'j'}^{k'}}{d^{n-1}\hat{p}_3}\right\} \Gamma_{j'j}^{(S)}(z_2,\epsilon)\Gamma_{i'i}^{(S)}(z_1,\epsilon)\right] \tag{4.4}$$

where the short distance cross-section $\hat{\sigma}$ is evaluated at rescaled values of the parton-momenta,

$$\hat{p}_1 = z_1 p_1, \qquad \hat{p}_2 = z_2 p_2, \qquad \hat{p}_3 = p_3/z_3. \tag{4.5}$$

To first order in α_S the singular parts of the functions $\Gamma^{(S,T)}$ are equal and given by the Altarelli-Parisi functions. At this order we may define the functions $\Gamma^{(S,T)}$ to be,

$$\Gamma_{ii'}^{(1)}(z,\epsilon) = \delta_{ii'}\delta(1-z) - \frac{\alpha_S}{2\pi} P_{ii'}(z)\left(\frac{1}{\epsilon} + \ln(4\pi) - \gamma_E\right) \tag{4.6}$$

The singularities from the collinear emission of partons appear as poles in ϵ. The association of the $\ln(4\pi)$ and Euler constant with the pole in ϵ defines this to be the $\overline{MS}$ type of mass singularity factorisation. Unless otherwise stated this is the factorisation used everywhere in this section.

As indicated in the previous sections, the parton cross-sections σ are calculated by averaging over $n-2$ spin states of initial gluons. This is to be constrasted with refs.[1 − 3] where averages were performed over 2 spin states of initial gluons. The results of refs.[1 − 3] therefore differ in a simple, calculable way from the results of the present paper [1]. In the notation of this paper it corresponds to performing the spin averages as we do here but making the replacement in Eq.(4.4), (for the case of incoming gluons, denoted by g.)

$$\Gamma^{(S)}_{jg}(z,\epsilon) \rightarrow \frac{1}{(1-\epsilon)}\left[\delta_{jg}\delta(1-z) - \frac{\alpha_S}{2\pi}P_{jg}(z)(\frac{1}{\epsilon} + \ln(4\pi) - \gamma_E) + O({\alpha_S}^2)\right] \quad (4.7)$$

Eq.(4.7) makes it clear that this replacement corresponds to a different factorisation prescription. Of course, physical results must be independent of the choice of factorisation scheme. Such a modification of the singular function Γ at order α_S, leads to a modification of the two loop Altarelli-Parisi function in such a way that physical results are independent of the choice of factorisation scheme. The choice made in Eq.(4.6) is in accord with the normal choice made for the two-loop anomalous dimensions,(see for example ref.[17]).

In ref.[1] the factorisation scheme was modified so that direct comparison could be made with parton distribution and decay functions taken respectively from deep inelastic scattering and deep inelastic e^+e^- annihilation. By using the distribution and decay functions measured in these processes at the appropriate scale μ^2, this factorisation scheme leads directly to physical predictions for one hadron inclusive scattering. The particular modifications of eq.(4.4) used in ref.[1] were,

$$\Gamma^{(S)}_{qq}(z,\epsilon) = \Gamma^{(1)}_{qq}(z,\epsilon) + \frac{\alpha_S}{2\pi}f_{qq}(z) + O({\alpha_S}^2)$$

$$\Gamma^{(S)}_{gq}(z,\epsilon) = \Gamma^{(1)}_{gq}(z,\epsilon) + \frac{\alpha_S}{2\pi}f_{gq}(z) + O({\alpha_S}^2)$$

$$\Gamma^{(T)}_{qq}(z,\epsilon) = \Gamma^{(1)}_{qq}(z,\epsilon) + \frac{\alpha_S}{2\pi}d_{qq}(z) + O({\alpha_S}^2) \quad (4.8)$$

[1] This issue has been discussed in ref.[22].

The finite $O(\alpha_S)$ corrections are given by[11,23,24],

$$f_{qq}(z) = \frac{V}{2N}\left((1+z^2)\left[\frac{\ln(1-z)}{1-z}\right]_+ - \frac{3}{2}\left[\frac{1}{1-z}\right]_+ - \frac{(1+z^2)}{1-z}\ln(z) \right.$$
$$\left. +3+2z-(\frac{9}{2}+\frac{\pi^2}{3})\delta(1-z)\right) \tag{4.9}$$

$$d_{qq}(z) = \frac{V}{2N}\left((1+z^2)\left[\frac{\ln(1-z)}{1-z}\right]_+ - \frac{3}{2}\left[\frac{1}{1-z}\right]_+ + 2\frac{(1+z^2)}{1-z}\ln(z) \right.$$
$$\left. +\frac{3}{2}(1-z)+(\frac{2\pi^2}{3}-\frac{9}{2})\delta(1-z)\right) \tag{4.10}$$

In ref.[1] various simple forms for f_{gq} were investigated. In this paper we will set $f_{gq}=0$. We shall refer to this type of factorisation as the 'physical scheme'.

To analyse the inclusive hadronic cross-section numerically it is useful to introduce the dimensionless functions $\rho^H, \hat{\rho}, \phi^H$ and $\hat{\phi}$.

$$E_3\frac{d^3\sigma^H}{d^3P_3} = \frac{1}{P_T^4}\,\rho^H(\tau_1^H,\tau_2^H,\Lambda^2/S) = \frac{1}{P_T^4}\,\phi^H(\tau_1^H,\tau_2^H,\Lambda^2/P_T^2)$$

$$\hat{p}_3^0\frac{d^3\hat{\sigma}_{i'j'}^{k'}}{d^3\hat{p}_3} = \frac{1}{p_T^4}\,\hat{\rho}(\hat{\tau}_1,\hat{\tau}_2,\mu^2/s) = \frac{1}{p_T^4}\,\hat{\phi}(\hat{\tau}_1,\hat{\tau}_2,\mu^2/p_T^2). \tag{4.11}$$

We have introduced the rescaled hadronic and partonic variables

$$\tau_1^H = \frac{P_1.P_3}{P_1.P_2},\ \tau_2^H = \frac{P_2.P_3}{P_1.P_2},\ \ \hat{\tau}_1 = \frac{p_1{\cdot}p_3}{p_1{\cdot}p_2},\ \hat{\tau}_2 = \frac{p_2{\cdot}p_3}{p_1{\cdot}p_2} \tag{4.12}$$

such that,

$$P_T^2 = \tau_1^H\tau_2^H S,\ \ p_T^2 = \hat{\tau}_1\hat{\tau}_2 s. \tag{4.13}$$

The dependence of the function ρ^H on the variable S, (or of the function ϕ^H on P_T), at fixed τ_1^H, τ_2^H provides a measure of the departure from strictly point-like behaviour. From Eq.(4.2) it follows that the observed hadronic ρ^H is predicted in terms of the short distance $\hat{\rho}$,

$$\rho^H(\tau_1^H,\tau_2^H,\Lambda^2/S) = \sum_{i,j,k}\int_0^1 dx_1dx_2dx_3d\hat{\tau}_1d\hat{\tau}_2\; x_1x_2x_3^4\;\delta(\tau_1^H-\hat{\tau}_1x_2x_3)$$
$$\delta(\tau_2^H-\hat{\tau}_2x_1x_3)\left[D_k^{H_3}(x_3,\mu^2)\left\{\hat{\rho}_{ij}^k(\hat{\tau}_1,\hat{\tau}_2,\mu^2/s)\right\}F_j^{H_2}(x_2,\mu^2)F_i^{H_1}(x_1,\mu^2)\right] \tag{4.14}$$

A similar formula relates ϕ^H and $\hat{\phi}$. In the order of perturbation theory to which we are working $\hat{\rho}$ has the following structure,

$$\begin{aligned}\hat{\rho}\left(\hat{\tau}_1,\hat{\tau}_2,\frac{\mu^2}{s}\right) &= \left(\frac{\alpha_S(\mu^2)}{2\pi}\right)^2 \Big\{\hat{\rho}_0(\hat{\tau}_1)\delta(1-\hat{\tau}_1-\hat{\tau}_2) \\ &+\theta(1-\hat{\tau}_1-\hat{\tau}_2)\left(\frac{\alpha_S(\mu^2)}{2\pi}\right)\left[\hat{\rho}_1(\hat{\tau}_1,\hat{\tau}_2)+\hat{\rho}_1'(\hat{\tau}_1,\hat{\tau}_2)\ln\left(\frac{\mu^2}{s}\right)\right]\Big\}\end{aligned} \tag{4.15}$$

and $\hat{\phi}$ is given by,

$$\begin{aligned}\hat{\phi}\left(\hat{\tau}_1,\hat{\tau}_2,\frac{\mu^2}{p_T^2}\right) &= \left(\frac{\alpha_S(\mu^2)}{2\pi}\right)^2 \Big\{\hat{\phi}_0(\hat{\tau}_1)\delta(1-\hat{\tau}_1-\hat{\tau}_2) \\ &+\theta(1-\hat{\tau}_1-\hat{\tau}_2)\left(\frac{\alpha_S(\mu^2)}{2\pi}\right)\left[\hat{\phi}_1(\hat{\tau}_1,\hat{\tau}_2)+\hat{\phi}_1'(\hat{\tau}_1,\hat{\tau}_2)\ln\left(\frac{\mu^2}{p_T^2}\right)\right]\Big\}\end{aligned} \tag{4.16}$$

where,

$$\begin{aligned}\hat{\phi}_0(\hat{\tau}_1) &= \hat{\rho}_0(\hat{\tau}_1) \\ \hat{\phi}_1(\hat{\tau}_1,\hat{\tau}_2) &= \hat{\rho}_1(\hat{\tau}_1,\hat{\tau}_2)+\hat{\rho}_1'(\hat{\tau}_1,\hat{\tau}_2)\ln(\hat{\tau}_1\hat{\tau}_2) \\ \hat{\phi}_1'(\hat{\tau}_1,\hat{\tau}_2) &= \hat{\rho}_1'(\hat{\tau}_1,\hat{\tau}_2)\end{aligned} \tag{4.17}$$

Note that the physical cross-section is independent of the renormalisation point μ.

$$\mu^2\frac{d}{d\mu^2}\,\rho^H(\tau_1^H,\tau_2^H,\Lambda^2/S) = 0 \tag{4.18}$$

Thus inserting the form of Eq.(4.15) into Eq.(4.14) and using Eq.(2.10), we find that $\hat{\rho}_1'$ is completely determined by renormalisation group arguments.

$$\begin{aligned}\hat{\rho}'^{\,k}_{1ij}(\hat{\tau}_1,\hat{\tau}_2) = \Big\{&2b_0\,\hat{\rho}^{\,k}_{0ij}(\hat{\tau}_1) - \hat{z}_3^3 P_{kk'}(\hat{z}_3)\,\hat{\rho}^{\,k'}_{0ij}\Big(\frac{\hat{\tau}_1}{\hat{\tau}_1+\hat{\tau}_2}\Big) \\ &-\frac{\hat{z}_2}{1-\hat{\tau}_2}\hat{\rho}^{\,k}_{0ij'}(1-\hat{\tau}_2)\,P_{j'j}(\hat{z}_2) - \frac{\hat{z}_1}{1-\hat{\tau}_1}\hat{\rho}^{\,k}_{0i'j}(\hat{\tau}_1)\,P_{i'i}(\hat{z}_1)\Big\}\end{aligned} \tag{4.19}$$

where

$$\hat{z}_1 = \frac{\hat{\tau}_2}{1-\hat{\tau}_1}, \qquad \hat{z}_2 = \frac{\hat{\tau}_1}{1-\hat{\tau}_2}, \qquad \hat{z}_3 = \hat{\tau}_1+\hat{\tau}_2 \tag{4.20}$$

Following ref.[2, 3] we may define moments of the hadronic and partonic cross-sections,

$$f(n,m) = \int_0^1 d\tau_1 \int_0^1 d\tau_2\; \tau_1^{n-1}\tau_2^{m-1} f(\tau_1,\tau_2)$$

$$F(n) = \int_0^1 dx\, x^{n-1} F(x) \tag{4.21}$$

Because of the simple structure of the s dependence in Eqs.(4.15,4.16) we find, after taking moments at fixed S or at fixed P_T, that the factorisation of the long and short distance parts of becomes manifest.

$$\begin{aligned}
\rho^H\left(n, m, \frac{\Lambda^2}{S}\right) &= \sum_{i,j,k}\Big[D_k^{H_3}(n+m+3,\mu^2)\left\{\hat\rho_{ij}^k\left(n, m, \frac{\mu^2}{\hat s(n,m,\mu)}\right)\right\} \\
&\qquad F_j^{H_2}(n+1,\mu^2)F_i^{H_1}(m+1,\mu^2)\Big] \\
\phi^H\left(n, m, \frac{\Lambda^{2\,2}}{P_T}\right) &= \sum_{i,j,k}\Big[D_k^{H_3}(n+m+3,\mu^2)\left\{\hat\phi_{ij}^k\left(n, m, \frac{\mu^2}{\hat p_T(n,m,\mu)}\right)\right\} \\
&\qquad F_j^{H_2}(n+1,\mu^2)F_i^{H_1}(m+1,\mu^2)\Big]
\end{aligned} \tag{4.22}$$

Thus by considering the moments of $\hat\rho$ and $\hat\phi$ we can obtain information about the $O(\alpha_S{}^3)$ corrections, almost without reference to the form of the distribution functions.

Taking moments of Eq.(4.15) we find,

$$\begin{aligned}
&\hat\rho\left(n, m, \frac{\mu^2}{\hat s(n,m,\mu)}\right) = \\
&\left(\frac{\alpha_S}{2\pi}\right)^2\left\{\hat\rho_0(n,m) + \left(\frac{\alpha_S}{2\pi}\right)\left[\hat\rho_1(n,m) + \hat\rho_1'(n,m)\ln\left(\frac{\mu^2}{\hat s(n,m,\mu)}\right)\right]\right\}
\end{aligned} \tag{4.23}$$

The only dependence on the form of the distribution and decay functions enters through $\hat s$ which is defined as,

$$\hat s(n,m,\mu) = S\exp\left\{\frac{d}{dm}\ln F_i^{H_1}(m+1,\mu^2) + \frac{d}{dn}\ln F_j^{H_2}(n+1,\mu^2)\right\} \tag{4.24}$$

The function $\hat s$ describes the effective parton sub-energy for the process as a function of the hadronic energy, $S = (P_1 + P_2)^2$ and the moment number.

Similarly Eq.(4.16) implies,

$$\begin{aligned}
&\hat\phi\left(n, m, \frac{\mu^2}{\hat p_T^2(n,m,\mu)}\right) = \\
&\left(\frac{\alpha_S}{2\pi}\right)^2\left\{\hat\phi_0(n,m) + \left(\frac{\alpha_S}{2\pi}\right)\left[\hat\phi_1(n,m) + \hat\phi_1'(n,m)\ln\left(\frac{\mu^2}{\hat p_T^2(n,m,\mu)}\right)\right]\right\}
\end{aligned} \tag{4.25}$$

where p_T is given by,

$$\hat{p}_T^2(n,m,\mu) = P_T^2 \exp\left\{-2\frac{d}{dJ}\ln D_k^{H_3}(J,\mu^2)\right\}\Big|_{J=n+m+3} \tag{4.26}$$

Eqs.(4.23) and (4.25) are well suited for the simple numerical estimates which we wish to perform in this section. If the short distance cross-section is dominated by one parton subprocess the analysis of the size of the correction can be performed without introducing particular forms for the distribution or decay functions. The corrections to $\hat{\rho}(n,m)$ and $\hat{\phi}(n,m)$ can then be used to give an estimate of the size of correction to the hadronic cross-section.

The results given in Sections II and III put a complete analysis of the $O(\alpha_S{}^3)$ results for one particle inclusive cross-sections including all parton subprocesses within our grasp. As indicated in the introduction we find this of limited experimental interest and we choose not to do it at the present time. We will instead consider only the three short distance cross-sections derived from the following parton subprocesses.

$$\begin{array}{lll} (1) & q_j + q_k \to q_j + X & j \neq k \\ (2) & q_j + q_k \to g + X & j \neq k \\ (3) & g + g \to g + X & \end{array} \tag{4.28}$$

We consider processes (1) and (2) because analytic results for them have already appeared in the literature. Process (3) is included because, in an imaginary world in which there are no quarks, it can be analysed on its own.

Firstly we consider the comparison with the work of other authors. Explicit analytic results for the short-distance cross-sections $\hat{\sigma}$ for process (1) have been presented in refs.[$1-3$]. We are in agreement with these analytic results of these references, after taking into account the modifications of the factorisation prescription described above [2]. However we are not in agreement with the analytic results for process (2) given in ref.[25]. The formulae for the short distance cross-sections for processes (2) and (3) are of about the same length as the formula given for process (1) in refs.[$1-3$]. We choose not to present them.

[2] We believe that the entry for D_{300} and D_{400} in the apppendix of ref.[3] contains a misprint and should read $D_{300} = D_{400} = \pi^2(\frac{1}{2}C_A - 2C_F)$.

In order to examine the size of the corrections we define the quantities,

$$r(n,m) = \frac{\hat{\rho}_1(n,m)}{\hat{\rho}_0(n,m)}, \qquad t(n,m) = \frac{\hat{\phi}_1(n,m)}{\hat{\phi}_0(n,m)}, \qquad t'(n,m) = \frac{\hat{\phi}'_1(n,m)}{\hat{\phi}_0(n,m)} \tag{4.29}$$

These quantities express the size of the higher order corrections relative to the lowest order corrections in units of $\alpha_S/(2\pi)$.

We consider first process (1). In Table. 8 we display the values of the ratios for the diagonal moments $n = m$. Note that for the 'natural' scale $\mu^2 = \hat{s}(n,m,\mu)$ the higher order corrections are large and positive. For any given moment it is always possible to choose a scale such that the higher order corrections vanish. For each moment we define the ratios $\eta_r(n,m)$ and $\eta_t(n,m)$

$$\eta_r(m,n) = \frac{\mu^2}{\hat{s}(n,m,\mu)}, \qquad \eta_t(m,n) = \frac{\mu^2}{\hat{p}_T^2(n,m,\mu)} \tag{4.30}$$

The values of the ratios which we must choose to ensure the vanishing of the higher order corrections are shown in Table 8.

Introducing the physical factorisation scheme of Eqs.(4.8) makes the modifications

$$r \to r^c, \quad t \to t^c. \tag{4.31}$$

In the physical scheme the size of the corrections is substantially reduced. Table 8 also shows the value of η_t^c which leads to the vanishing of the higher corrections in the physical scheme. This value is approximately equal to $\frac{1}{4}$ for all the diagonal moments listed. Identifying $\hat{p}_T$ with the whole transverse energy of a jet E_T suggests that jet cross-sections can be well described by setting the effective scale $\mu^2 = E_T^2/4$ and including only the lowest order cross-section. This approach has often been used in practical calculations, for lack of more reliable information. Whether in fact this a correct inference from information on one particle inclusive cross-sections and whether this pattern is maintained for all parton subprocesses will have to await further investigation. In the meantime we point out that neither the information on the angular distribution which we present below nor the earlier work on jet cross-sections[5] support this approximation.

In order to get a feeling for the significance of the double moments, it is useful to perform a change of variables. In terms of the variables $x = 2E_3/\sqrt{S}$ and the centre of mass scattering angle ($z = \cos\theta_{CM}$), we have,

$$\tau_1^H = x\left(\frac{1-z}{2}\right), \qquad \tau_2^H = x\left(\frac{1+z}{2}\right) \tag{4.32}$$

The moments of ϕ^H may be written,($L = n + m$),

$$\phi^H\left(n, m, \frac{\Lambda^2}{P_T^2}\right) = \int_0^1 dx\, x^{L-1} \int_{-1}^1 dz\, \left(\frac{1-z}{2}\right)^{n-1}\left(\frac{1+z}{2}\right)^{m-1} \phi^H\left(\tau_1^H, \tau_2^H, \frac{\Lambda^2}{P_T^2}\right) \tag{4.33}$$

At fixed transverse momentum the integer L corresponds to variations in the beam energy, whereas $\bar{z} = (m-n)(n+m)$ describes the angular dependence of ϕ^H. Figs.(10),(11) and (12) show the angular dependence of the correction as a function of $\bar{z}$. We see that $t(n,m)$ shows appppreciable dependence on $\bar{z}$ which is not present in $t_1'(n,m)$. Thus it is not possible to define a universal η which removes the correction for all angles. This is shown in Fig.(12). At fixed L the value of η_t varies as function of $\bar{z}$. Of course in a real physical situation we might expect to find partons of a given type inside both beam and target hadrons. This makes Figs.(10,11) symmetric and tends to reduce the angular dependence. Note also that the value of $\bar{z}$ determines the region in z which contributes most significantly to the moment integral Eq(4.33).

$$z \approx \frac{\bar{z}}{(1-2/L)} \tag{4.34}$$

Thus the large values of $|\bar{z}|$ where the angular variation is biggest correspond to angles close to the beam direction which may not be observable experimentally. Nevertheless the conclusion for this process is that higher order effects vary significantly as a function of angle. As a final illustration of this in Fig.(13) we show η_t^c in the physical factorisation scheme. We find that η_t^c deviates significantly from $\frac{1}{4}$ in the forward direction.

In Table 9 we show the diagonal moments of the quantities r, t and t' for process (2). Table 9 serves to document our differences with the results of ref.[25].

Lastly we consider process (3) in a hypothetical world without quarks. To do this we everywhere set $T_R = 0$, (including in the definition of the beta function Eq.(2.11)). Since there are now no other processes with which process (3) can mix we can consider it by itself. Table 10 diplays the results for the diagonal moments. The corrections are large and positive, but the values of η_r and η_t which minimise the higher order correction are of a similar order of magnitude to the values found for process (1). In this case there is at present no physical scheme calculated to sufficiently high order that we can use it to define the gluon distribution. This is because the gluon distribution function enters into deep inelastic scattering only at order α_S.

Figs.(14),(15) and (16) plot the change in t, t' and η_t with $\bar{z}$. Individually t and t' vary with $\bar{z}$ but the value of η_t which removes the higher order correction is almost independent of $\bar{z}$. The corrections to pure glue-glue scattering are practically independent of angle. The contrast between Fig.(16) and Figs.(12,13) is quite striking.

CONCLUSIONS.

We have presented results for all $2 \to 2$ and $2 \to 3$ parton scattering processes in QCD. The calculations were performed with massless quarks through to the sixth order in the strong coupling constant. Separately the $2 \to 2$ and $2 \to 3$ matrix elements are singular in the region of soft or collinear parton emission. These singularities cancel when they are combined to form physical observables. We have only done this in a limited number of cases.

The complexity of the calculations has led to this rather technical paper. It was our intention to present the results required in sufficient detail that they may be used for further elaboration by ourselves or by others.

We have performed a limited analysis of one hadron inclusive scattering. This provides a simple check of our results and allows us to make contact with earlier work. For the parton processes which we considered the corrections are large and positive. In other words the corrections can be reduced by choosing a renormalisation scale μ^2 substantially smaller than the 'natural' scales $\hat{s}$ or $\hat{p}_T^2$. The higher order corrections to inclusive cross-sections mediated by quark-quark scattering vary as a function of angle; the corrections to pure glue-glue scattering vary much less. The significance of these results for the jet cross-sections which are actually measured by modern detectors remains to be clarified.

We are confident that our results will aid the understanding of the most copious class of events in high energy hadron-hadron collisions at large transverse momentum.

ACKNOWLEDGMENTS

Discussions with I. Hinchliffe, D. Soper and M. Veltman have been helpful to this paper. Part of this work was carried out under the auspices of the Eugene workshop on Super-Collider physics. In addition, R.K.E. is grateful for the hospitality of the theory group at LBL.

REFERENCES

1. R. K. Ellis, M. A. Furman, H. E. Haber and I. Hinchliffe, Nucl. Phys. B173,(1980) 397.

2. W. Słomiński, Jagellonian University Thesis, Kraków, (1980).

3. W. Słomiński and W. Furmański, Kraków Preprint TPJU-11/81 (1981).

4. E. J. Eichten, I. Hinchliffe, K. D. Lane and C. Quigg, Rev. Mod. Phys. 56,(1984) 579.

5. M. A. Furman, Nucl. Phys. B197,(1981) 413,
   Phys. Lett. 98B,(1981) 99.

6. G. 't Hooft and M. Veltman, Nucl. Phys. B44,(1972) 189;
   C. G. Bollini and J.J. Giambiagi, Nuovo Cim. 12B,(1972) 20;
   W. J. Marciano, Phys. Rev. D12,(1975) 3861.

7. B. L. Combridge, J. Kripfganz and J. Ranft, Phys. Lett. 70B,(1977) 234.

8. M. A. Nowak, M. Praszałowicz and W. Słomiński, Munich preprint MPI-PAE/PTh 14/84 (1984).

9. M. Veltman, Schoonschip;
   H. Strubbe, Comp. Phys. Comm. 8,(1974) 1.

10. J. van der Bij and M. Veltman, Nucl. Phys. B231,(1984) 205.

11. W.A. Bardeen, A. Buras, D. W. Duke and T. Muta, Phys. Rev. D18, (1978) 3998.

12. D.J. Gross and F. Wilczek, Phys. Rev. Lett. 30, (1973) 1343;
    H. D. Politzer, Phys. Rev. Lett. 30, (1973) 1346.

13. W. Caswell, Phys. Rev. Lett. 33,(1974) 244;
    D. R. T. Jones, Nucl. Phys. B75,(1974) 531.

14. T. Gottschalk and D. Sivers, Phys. Rev. D21, (1980) 102;
    Z. Kunszt and E. Pietarinen, Nucl. Phys. B164,(1980) 45.

15. F. A. Berends R. Kleiss, P. de Causmaecker, R. Gastmans and T. T. Wu, Phys. Lett. 103B, (1981) 102.

16. G. Altarelli and G. Parisi, Nucl. Phys. B126,(1977) 298.

17. W. Furmański and R. Petronzio, Phys. Lett. 97B, (1980) 437, Z. Phys. C11, (1982) 293;
G. Curci, W. Furmański and R. Petronzio, Nucl. Phys. B175,(1980) 27.

18. E.G. Floratos, D. A. Ross and C. T. Sachrajda, Nucl. Phys. B129,(1977) 66, (E:B139,(1978) 545); Nucl. Phys. B152,(1979) 493.

19. A. Gonzalez-Arroyo, C. Lopez, and F. J. Yndurain, Nucl. Phys. B153,(1979) 161; Nucl. Phys. B159,(1979) 512.

20. R. K. Ellis, H. Georgi, M. Machacek, H. D. Politzer and G. G. Ross, Nucl. Phys. B152,(1979) 285.

21. D. Amati, G. Veneziano and R. Petronzio, Nucl. Phys. B146,(1978) 29.

22. J. Sheiman, Nucl. Phys. B152,(1979) 273;
D. W. Duke and J. F. Owens, Phys. Rev. D26, (1982) 1600.

23. G. Altarelli, R. K. Ellis and G. Martinelli, Nucl. Phys. B157,(1979) 461.

24. G. Altarelli, R. K. Ellis, G. Martinelli and S-Y Pi, Nucl. Phys. B160,(1979) 301;
R. Baier and K. Fey, Z. Phys. C2,(1979) 339.

25. M. A. Nowak and M. Praszałowicz, Acta. Phys. Polon. B15,(1984) 523.

Process $1+2 \to 3+4$	$\bar{\Sigma}\|M\|^2$
$q_j + q_k \to q_j + q_k$	$[a(s,t,u)]/(4N^2)$
$q_j + \bar{q}_k \to q_j + \bar{q}_k$	$[a(u,t,s)]/(4N^2)$
$q_j + \bar{q}_j \to \bar{q}_k + q_k$	$[a(t,s,u)]/(4N^2)$
$q_j + q_j \to q_j + q_j$	$[a(s,t,u)+a(s,u,t)+b(s,t,u)]/(4N^2)$
$q_j + \bar{q}_j \to q_j + \bar{q}_j$	$[a(u,t,s)+a(u,s,t)+b(u,t,s)]/(4N^2)$
$q_j + \bar{q}_j \to g + g$	$[c(s,t,u)]/(4N^2)$
$q_j + g \to q_j + g$	$-[c(t,s,u)]/(4(1-\epsilon)NV)$
$\bar{q}_j + g \to \bar{q}_j + g$	$-[c(t,u,s)]/(4(1-\epsilon)NV)$
$g + g \to q_j + \bar{q}_j$	$[c(s,t,u)]/(4(1-\epsilon)^2V^2)$
$g + g \to g + g$	$[d(s,t,u)]/(4(1-\epsilon)^2V^2)$

Table 1. Results for the $(2 \to 2)$ matrix elements in n dimensions summed and averaged over colours and spins.

$a^{(4)}(s,t,u)$	$2V\left(\frac{s^2+u^2}{t^2}-\epsilon\right)$
$b^{(4)}(s,t,u)$	$-\frac{4V}{N}(1-\epsilon)\left(\frac{s^2}{ut}+\epsilon\right)$
$c^{(4)}(s,t,u)$	$\frac{2V}{N}(1-\epsilon)\left(\frac{V}{ut}-\frac{2N^2}{s^2}\right)(t^2+u^2-\epsilon s^2)$
$d^{(4)}(s,t,u)$	$16VN^2(1-\epsilon)^2\left(3-\frac{ut}{s^2}-\frac{us}{t^2}-\frac{st}{u^2}\right)$

Table 2. The $O(g^4)$ approximations to the functions a, b, c and d for the $(2 \to 2)$ matrix elements in n dimensions.

Topology	Statistical Factor	Weight
1	$\frac{1}{2}$	1
2	1	2
3	1	1
4	1	1
Total No. of Interferences		5

Table 3. The statistical factors and weights with which the topologies $\Gamma^{(a)}$, of Fig. 4 enter in the process $q_j + q_k \to q_j + q_k$ at $O(\alpha_S{}^3)$.

Topology	Statistical Factor	Weight
1	$\frac{1}{2}$	2
2	1	4
3	1	2
4	1	2
Total No. of Interferences		10

Table 4. The statistical factors and weights with which the topologies $\Gamma^{(b)}$ of Fig. 5 enter in the process $q_j + q_j \to q_j + q_j$ at $O(\alpha_S{}^3)$.

Topology	Statistical Factor	Weight
1	$\frac{1}{2}$	2
2	1	4
3	1	2
4	$\frac{1}{2}$	2
5	1	4
6	1	2
7	1	2
8	$\frac{1}{2}$	2
9	1	4
10	1	2
11	1	1
12	$\frac{1}{2}$	2
13	$\frac{1}{2}$	2
14	1	2
15	1	2
16	1	2
17	$\frac{1}{2}$	1
18	$\frac{1}{2}$	1
19	1	1
20	1	1
21	1	1
Total No. of Interferences		42

Table 5. The statistical factors and weights with which the topologies $\Gamma^{(c)}$ of Fig. 7 enter in the process $q_j + \bar{q}_j \rightarrow g + g$ at $O(\alpha_S{}^3)$.

Topology	Statistical Factor	Weight
1	$\frac{1}{2}$	3
2	1	6
3	1	6
4	$\frac{1}{2}$	6
5	$\frac{1}{2}$	3
6	1	6
7	$\frac{1}{2}$	6
8	1	12
9	1	12
10	$\frac{1}{2}$	12
11	$\frac{1}{2}$	6
12	1	3
13	$\frac{1}{2}$	3
14	1	6
15	1	6
16	$\frac{1}{2}$	6
17	$\frac{1}{2}$	3
18	1	3
Total No. of Interferences		108

Table 6. The statistical factors and weights with which the topologies $\Gamma^{(d)}$ of Fig. 9 enter in the process $g + g \to g + g$ at $O(\alpha_S{}^3)$.

Process $1+2 \to 3+4+5$	$\bar{\Sigma}\,\|M\|^2$
$q_j + q_k \to q_j + q_k + g$	$[A(p_1, p_2, -p_3, -p_4, -p_5)]\,/(4N^2)$
$q_j + \bar{q}_k \to q_j + \bar{q}_k + g$	$[A(p_1, -p_4, -p_3, p_2, -p_5)]\,/(4N^2)$
$q_j + \bar{q}_j \to \bar{q}_k + q_k + g$	$[A(p_1, p_3, -p_2, -p_4, -p_5)]\,/(4N^2)$
$q_j + g \to q_j + q_k + \bar{q}_k$	$-\,[A(p_1, -p_5, -p_3, -p_4, p_2)]\,/(4N^2)$
$q_j + q_j \to q_j + q_j + g$	$[B(p_1, p_2, -p_3, -p_4, -p_5)]\,/(4N^2)$
$q_j + \bar{q}_j \to q_j + \bar{q}_j + g$	$[B(p_1, -p_4, -p_3, p_2, -p_5)]\,/(4N^2)$
$q_j + g \to q_j + q_j + \bar{q}_j$	$-\,[B(p_1, -p_5, -p_3, -p_4, p_2)]\,/(4(1-\epsilon)NV)$
$q_j + \bar{q}_j \to g + g + g$	$[C(p_1, p_2, -p_3, -p_4, -p_5)]\,/(4N^2)$
$q_j + g \to q_j + g + g$	$-\,[C(p_1, -p_3, p_2, -p_4, -p_5)]\,/(4(1-\epsilon)NV)$
$\bar{q}_j + g \to \bar{q}_j + g + g$	$-\,[C(-p_3, p_1, p_2, -p_4, -p_5)]\,/(4(1-\epsilon)NV)$
$g + g \to q_j + \bar{q}_j + g$	$[C(-p_3, -p_4, p_1, p_2, -p_5)]\,/(4(1-\epsilon)^2V^2)$
$g + g \to g + g + g$	$[D(p_1, p_2, -p_3, -p_4, -p_5)]\,/(4(1-\epsilon)^2V^2)$

Table 7. The matrix elements squared for the physical processes averaged over initial colours and spins in terms of the four basic functions A, B, C, D

n,m	r	r^c	t	t^c	t'	η_r	η_t	η_t^c
1,1	54.1	38.8	36.1	20.8	11.6	0.009	0.045	0.166
2,2	72.1	50.9	45.5	24.3	16.8	0.014	0.067	0.235
3,3	82.7	56.3	53.0	26.6	19.6	0.015	0.067	0.257
4,4	91.3	60.2	59.4	28.3	21.5	0.014	0.063	0.268
5,5	98.8	63.4	65.1	29.7	23.1	0.014	0.060	0.276
6,6	105.	66.2	70.1	31.0	24.3	0.013	0.056	0.279
7,7	111.	68.6	74.7	32.1	25.4	0.013	0.053	0.283
8,8	117.	70.8	79.0	33.1	26.4	0.012	0.050	0.285
9,9	122.	72.8	82.9	34.0	27.2	0.011	0.049	0.287
10,10	126.	74.7	86.6	34.9	28.0	0.011	0.045	0.288

Table 8. Diagonal moments of the radiative corrections to the process $q_j + q_k \rightarrow q_j + X$ at $O(\alpha_S{}^3)$. r, t and η as defined in Eqs.(4.29-4.31).

n,m	$r(n,m)$	$t(n,m)$	$t'(n,m)$	$\eta_r(n,m)$	$\eta_t(n,m)$
1,1	-39.7	-7.82	-9.38	0.015	0.43
2,2	-16.7	-6.52	-4.39	0.022	0.23
3,3	-11.3	-5.60	-2.86	0.019	0.14
4,4	-8.80	-4.94	-2.12	0.016	0.10
5,5	-7.36	-4.45	-1.69	0.013	0.07
6,6	-6.40	-4.06	-1.41	0.011	0.06
7,7	-5.69	-3.74	-1.21	0.009	0.05
8,8	-5.15	-3.48	-1.06	0.008	0.04
9,9	-4.72	-3.25	-0.94	0.007	0.03
10,10	-4.37	-3.06	-0.85	0.006	0.03

Table 9. Diagonal moments of the radiative corrections to the process $q_j+q_k \rightarrow g+X$ at $O(\alpha_S{}^3)$.

n, m	$r(n,m)$	$t(n,m)$	$t'(n,m)$	$\eta_r(n,m)$	$\eta_t(n,m)$
1,1	81.1	56.4	18.8	0.013	0.050
2,2	118.	74.3	29.2	0.018	0.079
3,3	141.	89.4	34.9	0.018	0.077
4,4	159.	103.	39.0	0.017	0.071
5,5	175.	114.	42.3	0.016	0.068
6,6	189.	125.	45.0	0.015	0.062
7,7	202.	135.	47.4	0.014	0.058
8,8	214.	144.	49.4	0.013	0.054
9,9	225.	152.	51.3	0.012	0.052
10,10	235.	160.	52.9	0.012	0.049

Table 10. Diagonal moments of the radiative corrections to the process $g+g \to g+X$ at $O(\alpha_S{}^3)$ in the limit $T_R = 0$.

FIGURE CAPTIONS

1. Feynman diagrams contributing to the $2 \to 2$ processes in order $O(g^2)$.

2. First radiative corrections to $q_j + q_k \to q_j + q_k$. The notation is as follows,

   Solid line: quark or anti-quark.

   Curly line: gluon, ghost or anti-ghost.

   Dashed line: gluon, ghost or anti-ghost, quark or anti-quark.

   The identification of the curly or dashed lines as detailed above is made in all possible ways consistent with,

   1) the conservation of ghost and quark number at every vertex

   2) the absence of four point vertices involving ghosts or quarks.

3. The five diagrams which are represented by diagram 1 of Fig. 2. In this diagram the curly line represents a gluon alone and the dotted line represents a ghost.

4. The independent topologies, $\Gamma^{(a)}$, obtained by interfering Fig. 1a with the five diagrams of Fig. 2.

5. The additional topologies, $\Gamma^{(b)}$, obtained by interfering Fig. 1b with the five diagrams of Fig. 2.

6. The first radiative corrections to the process $q_j + \bar{q}_j \to g + g$. Notation as in Fig. 2.

7. The independent topologies, $\Gamma^{(c)}$, obtained by interfering the diagrams of Fig. 1c with those of Fig. 6.

8. Diagrams contributing to the first radiative corrections to the process $g + g \to g + g$. The complete set of diagrams is obtained by adding diagrams obtained from the above by the exchanges $(p_1 \leftrightarrow p_3)$ and $(p_1 \leftrightarrow p_4)$. Notation as in Fig. 2.

9. The independent topologies, $\Gamma^{(d)}$, obtained by interfering the diagrams of Fig. 1d with those of Fig. 8.

10. $t(n,m)$ vs. $\bar{z} = (m-n)/(n+m)$ for various values of $L = n+m$ for quark-quark scattering. This illustrates the size and angular variation of the correction at the scale $\mu^2 = \hat{p}_T^2$.

11. $t'(n,m)$ vs. $\bar{z}$ showing the size and angular variation of the μ dependent part of the correction for quark-quark scattering.

12. $\eta_t(n,m)$ vs. $\bar{z}$. The effective scale needed to minimise the higher order correction to quark-quark scattering as a function of $\bar{z}$.

13. $\eta_t^c(n,m)$ vs. $\bar{z}$. The effective scale needed to minimise the higher order correction in the physical factorisation scheme.

14. $t(n,m)$ vs. $\bar{z}$. The size and angular variation of the correction at $\mu^2 = \hat{p}_T^2$ for gluon-gluon scattering.

15. $t'(n,m)$ vs. $\bar{z}$. The size and angular variation of the μ dependent part of the correction for gluon-gluon scattering.

16. $\eta_t(n,m)$ vs. $\bar{z}$. The effective scale needed to minimise the higher order correction to gluon-gluon scattering as a function of $\bar{z}$.

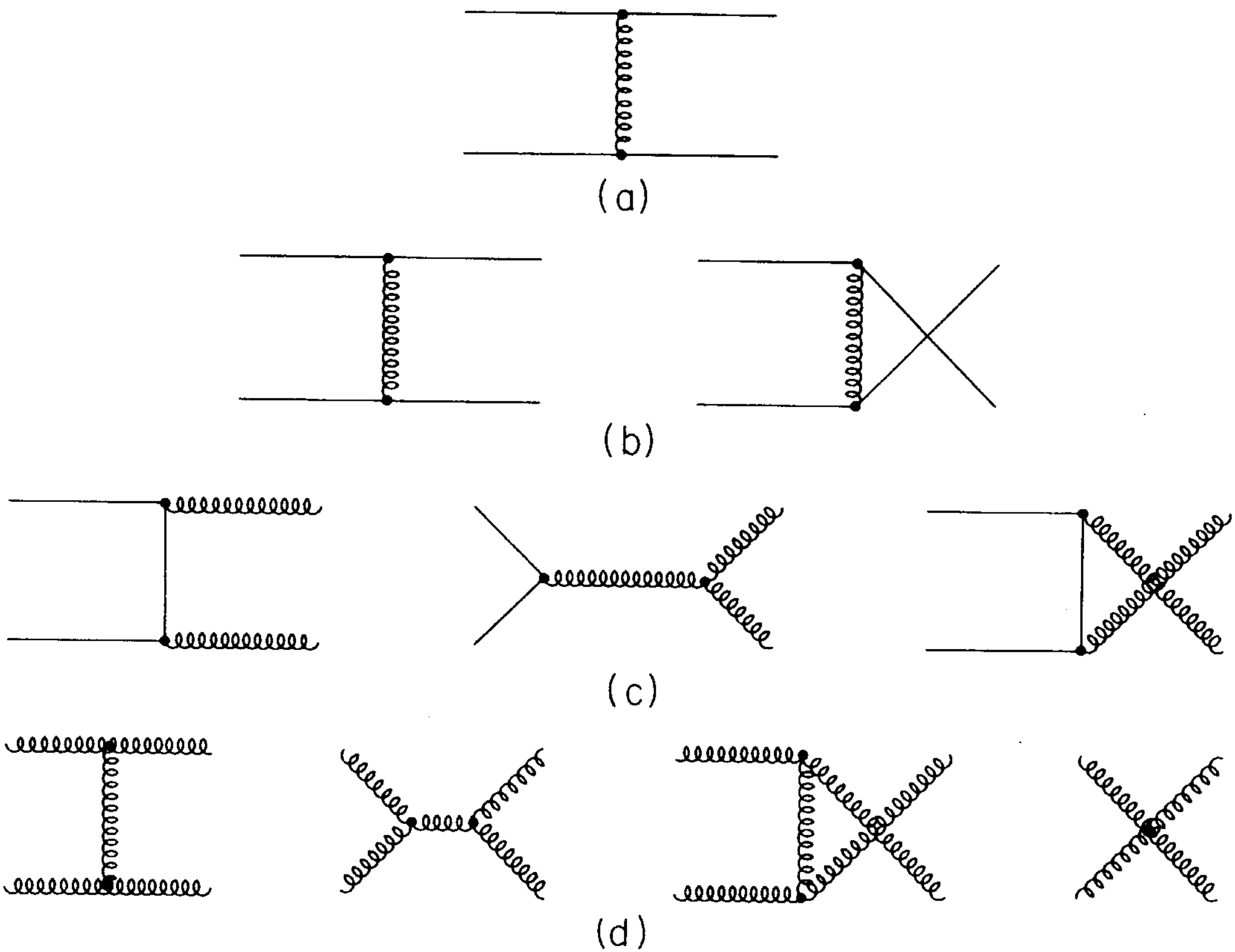

FIGURE 1

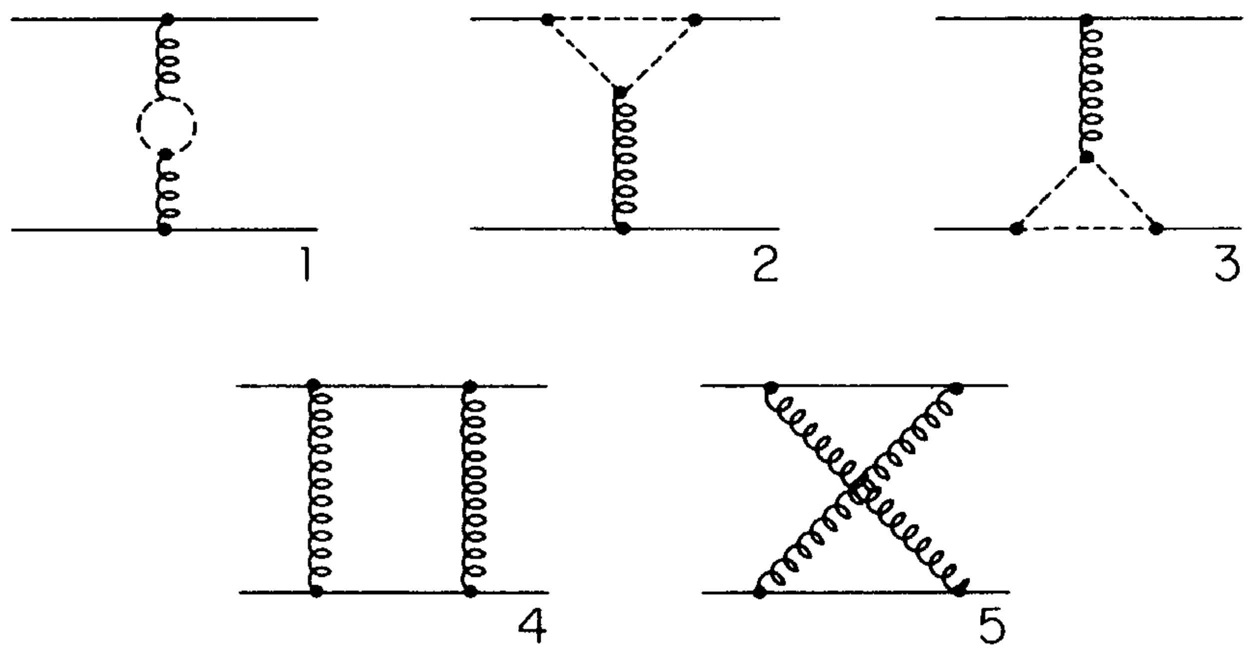

FIGURE 2

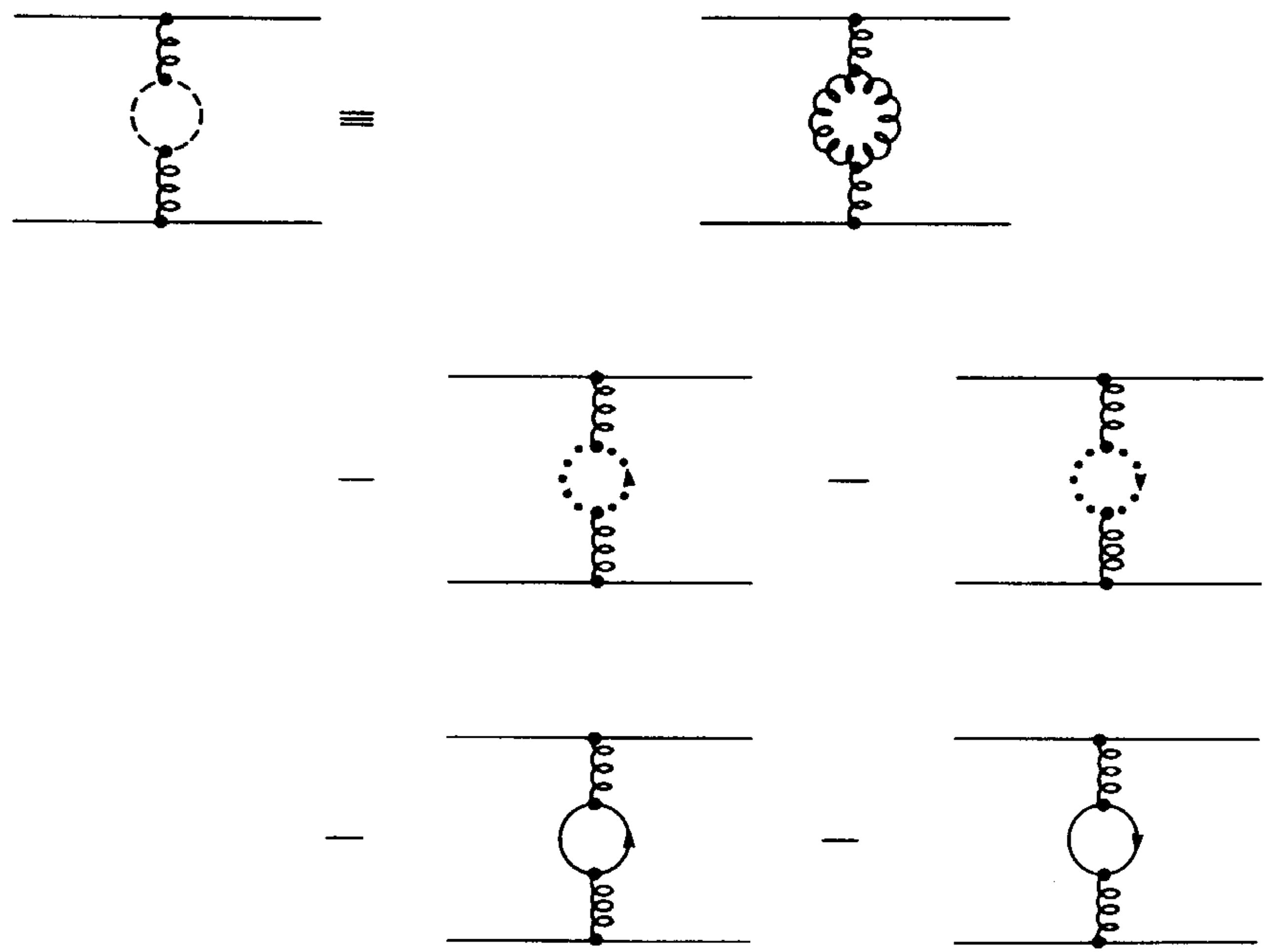

FIGURE 3

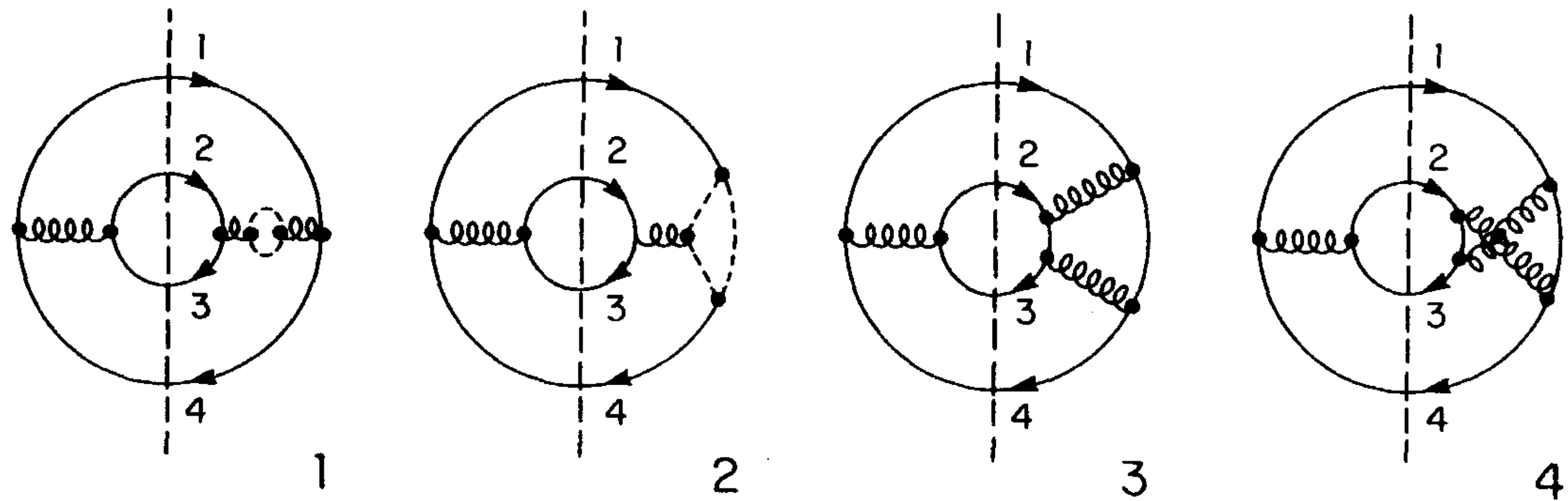

FIGURE 4

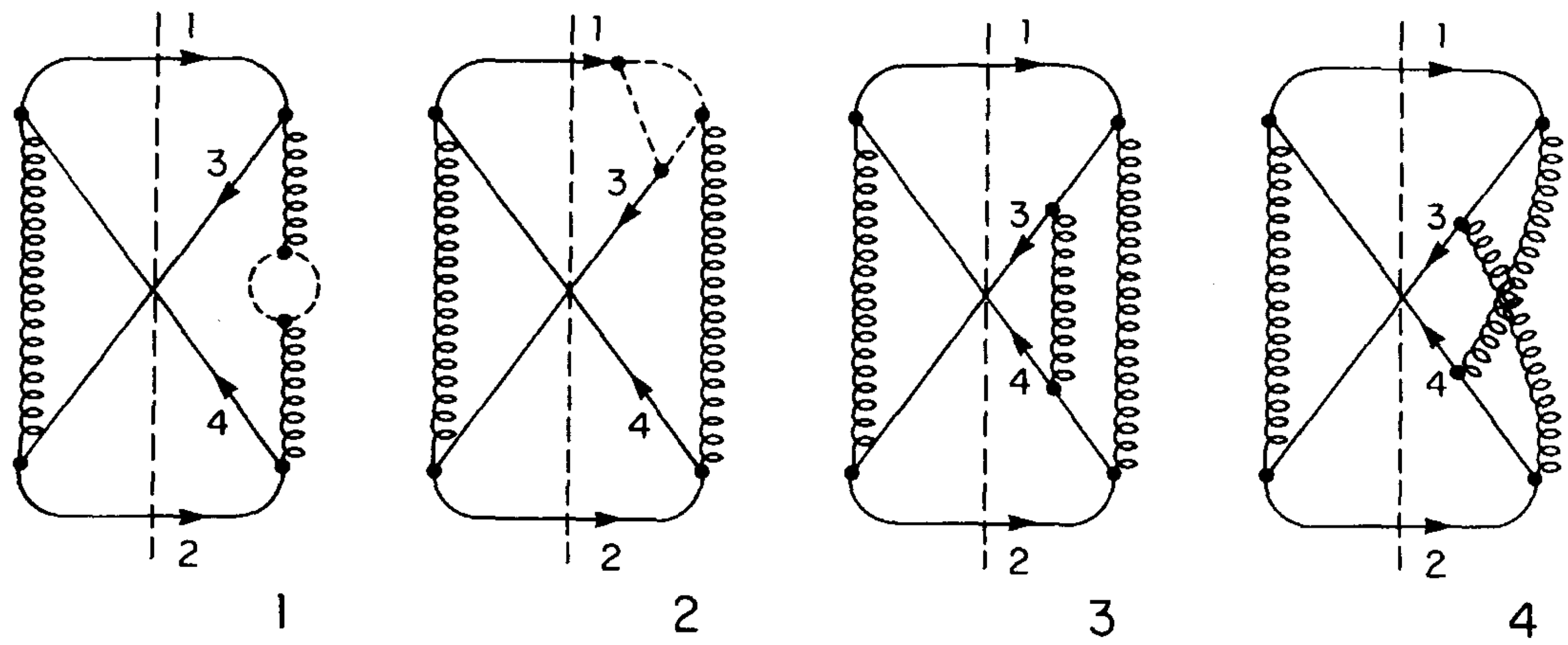

FIGURE 5

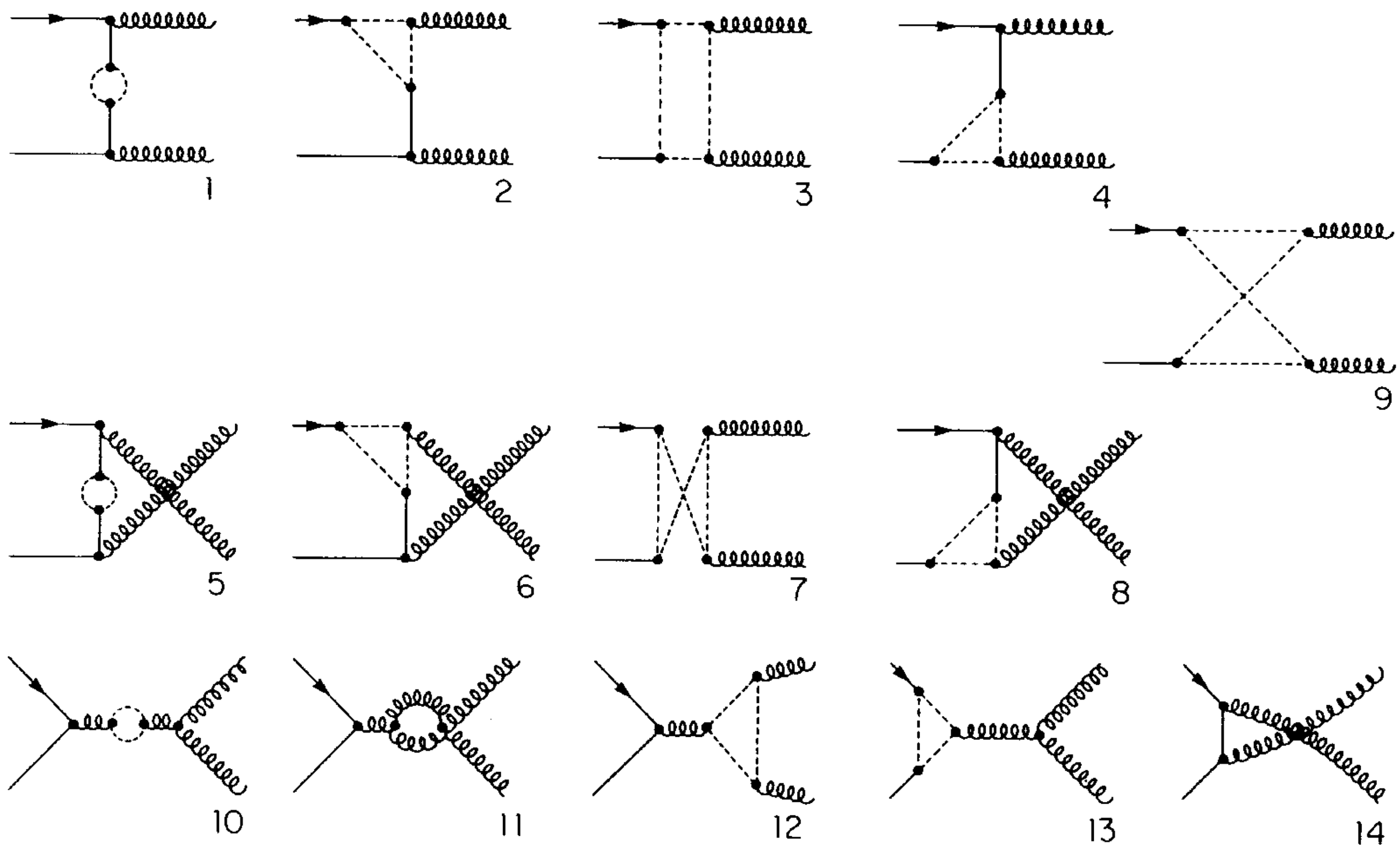

FIGURE 6

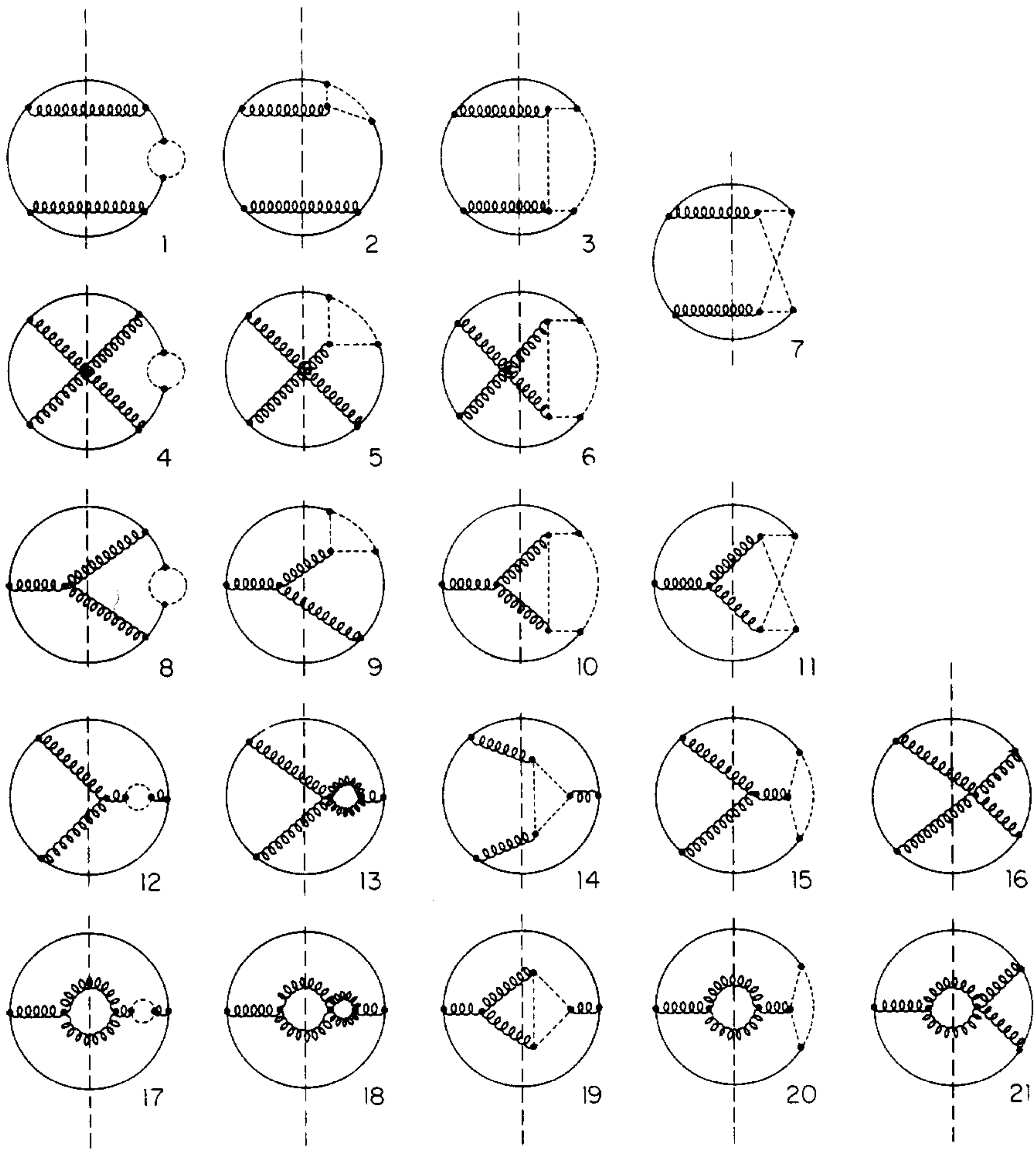

FIGURE 7

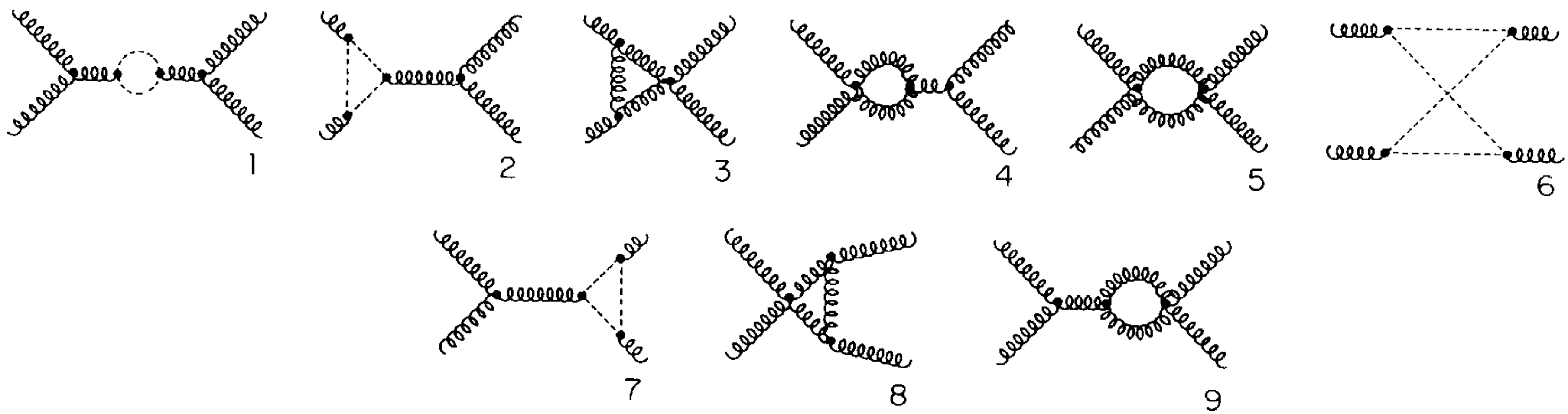

FIGURE 8

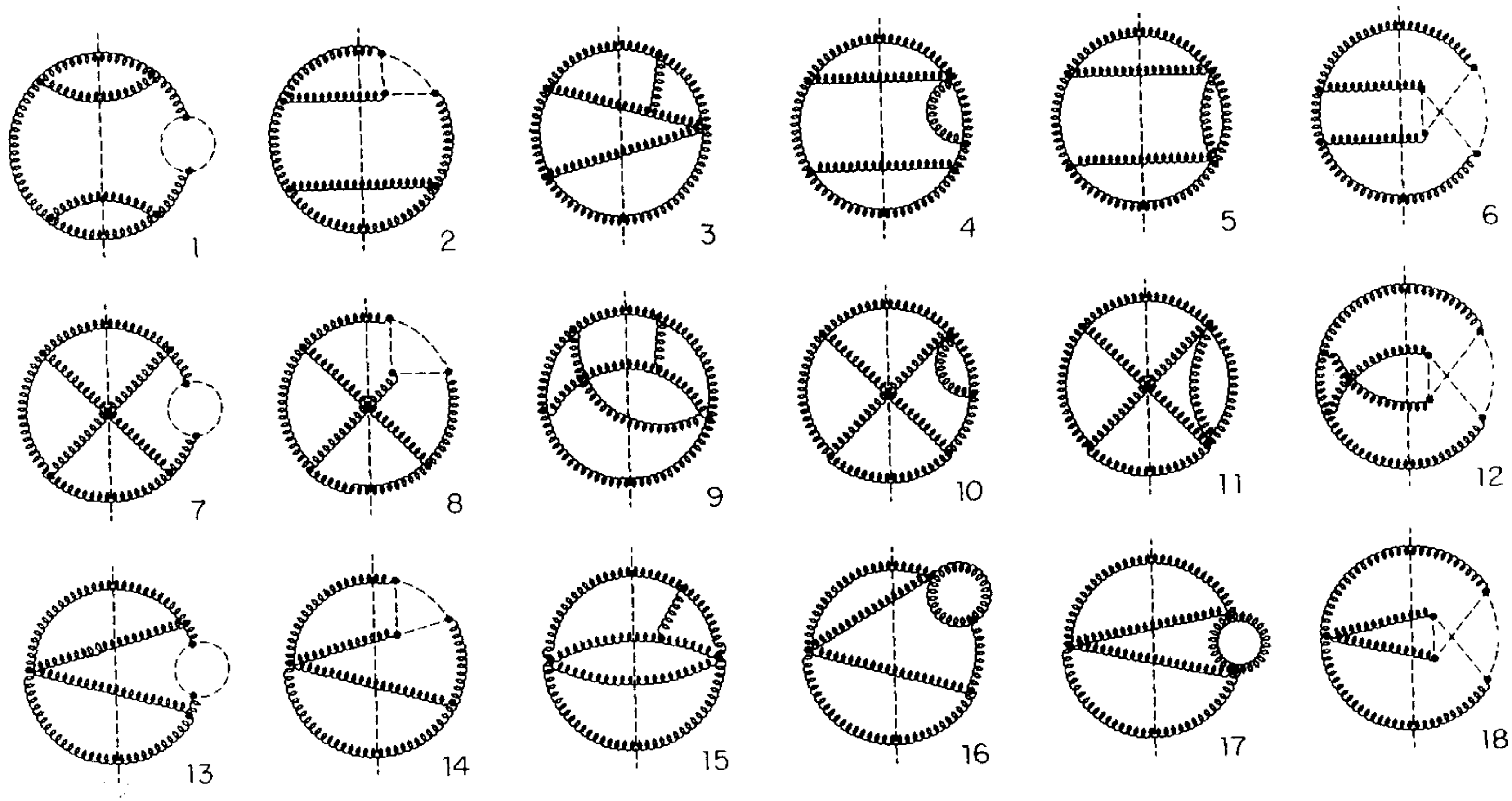

FIGURE 9

FIGURE 10

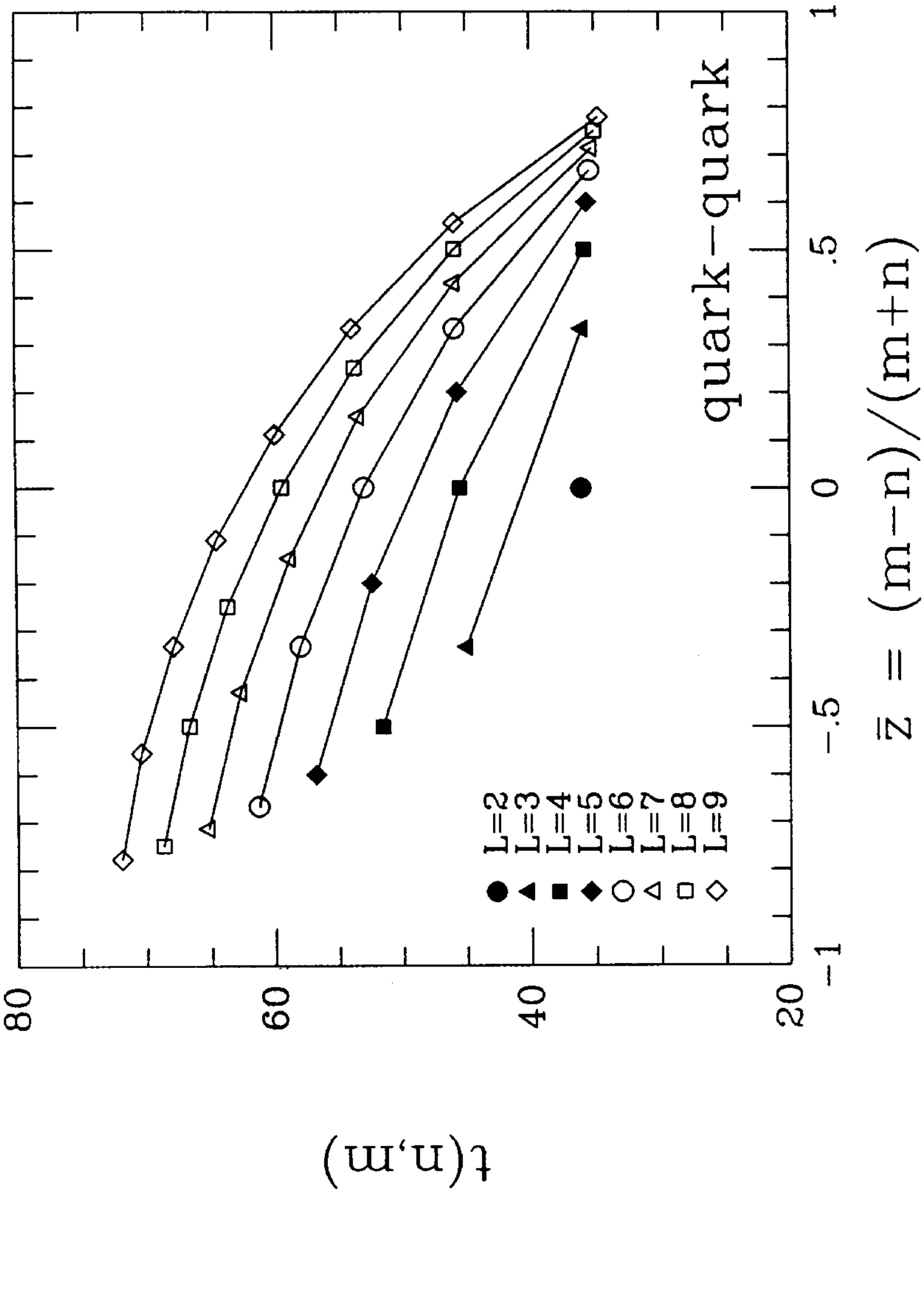

quark−quark
$\bar{z}$ = (m−n)/(m+n)
t(n,m)
L=2
L=3
L=4
L=5
L=6
L=7
L=8
L=9
−1
−.5
0
.5
1
20
40
60
80

FIGURE 11

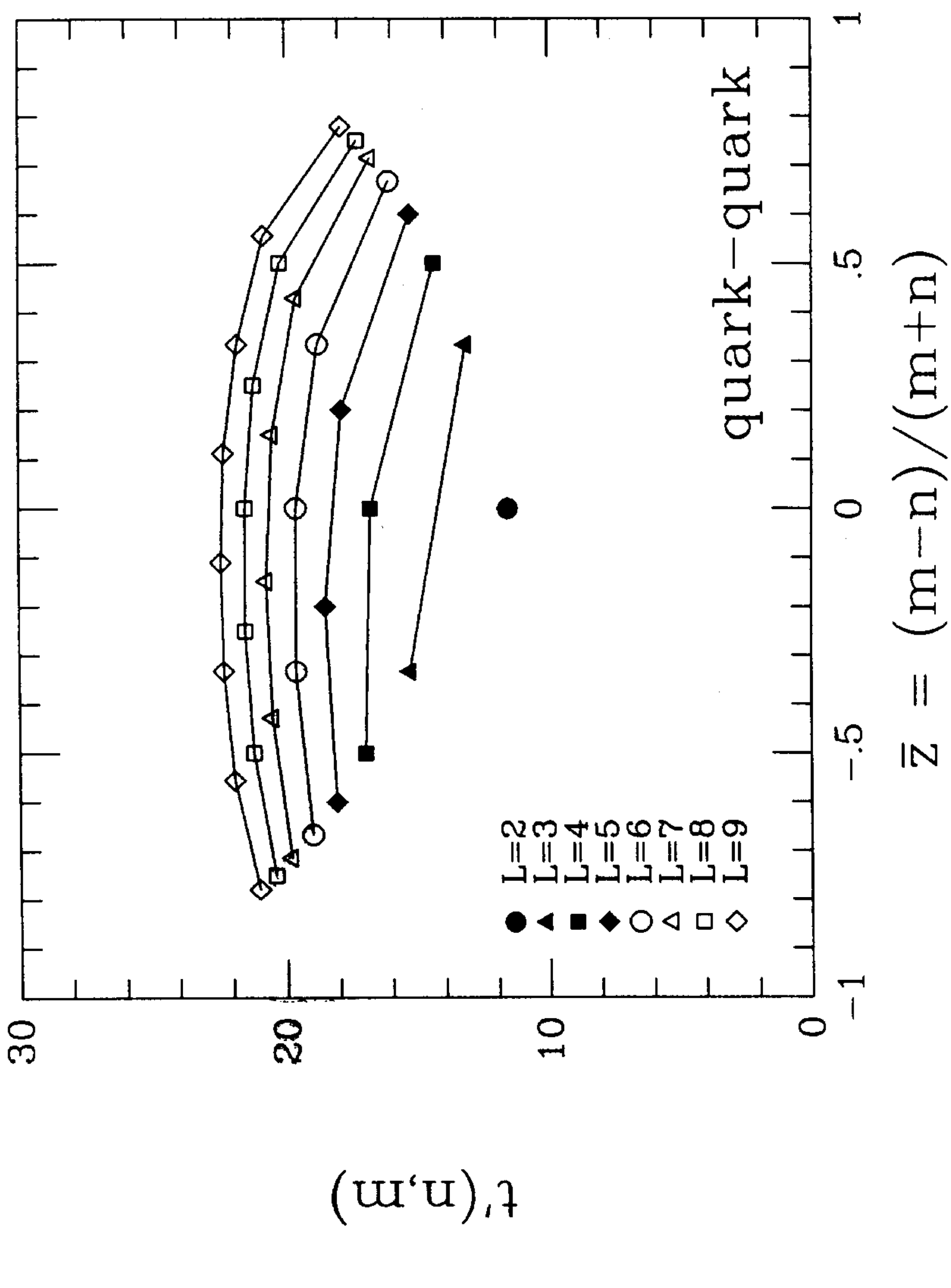

FIGURE 12

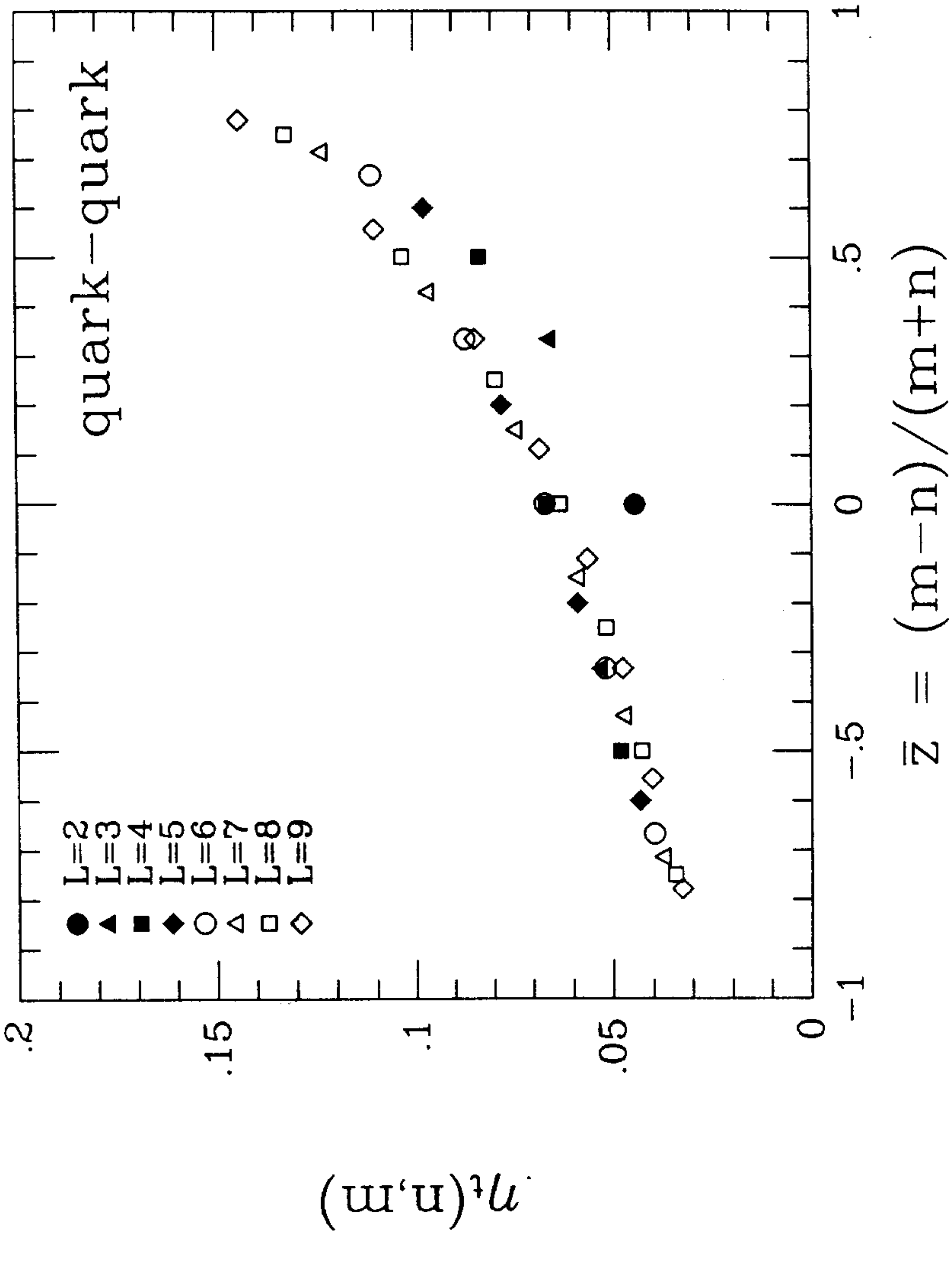

quark−quark
L=2
L=3
L=4
L=5
L=6
L=7
L=8
L=9
0
.05
.1
.15
.2
−1
−.5
0
.5
1
$\bar{z}$ = (m−n)/(m+n)
η_t(n,m)

FIGURE 13

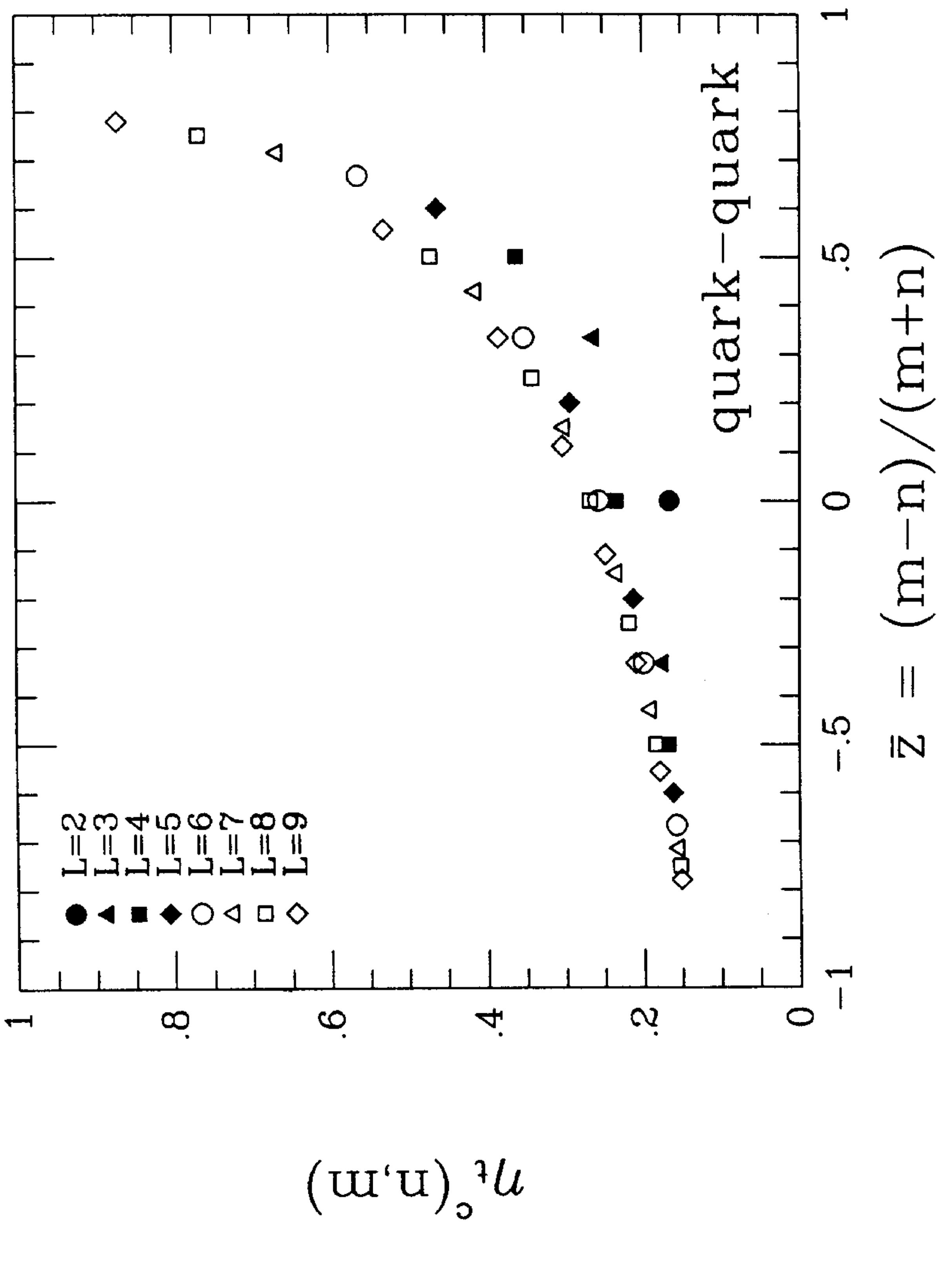

quark−quark
L=2
L=3
L=4
L=5
L=6
L=7
L=8
L=9
$\bar{z} = (m-n)/(m+n)$
$\eta_t^c(n,m)$
−1
−.5
0
.5
1
0
.2
.4
.6
.8
1

FIGURE 14

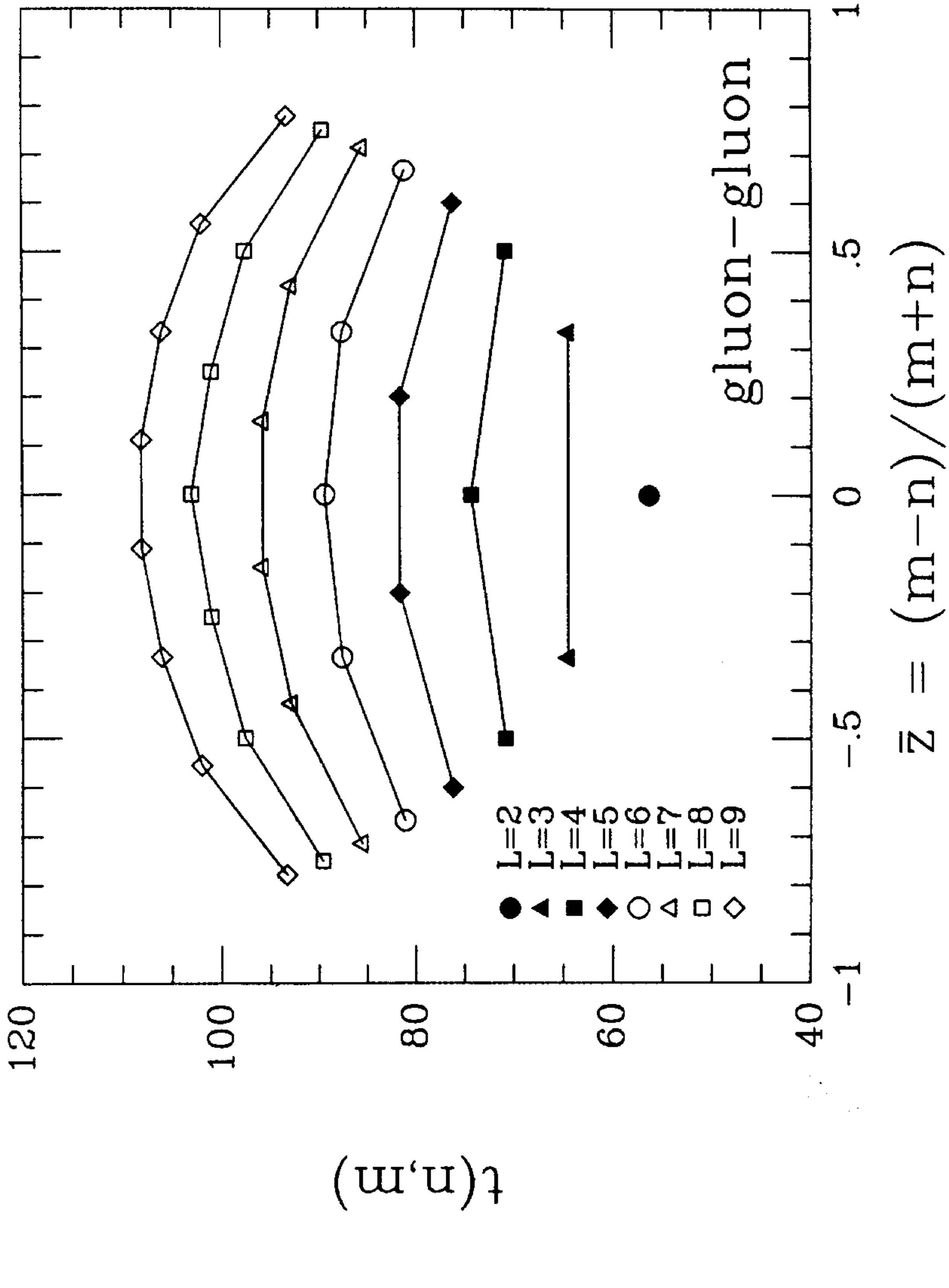

gluon−gluon
L=2
L=3
L=4
L=5
L=6
L=7
L=8
L=9
t(n,m)
z̄ = (m−n)/(m+n)
120
100
80
60
40
−1
−.5
0
.5
1

FIGURE 15

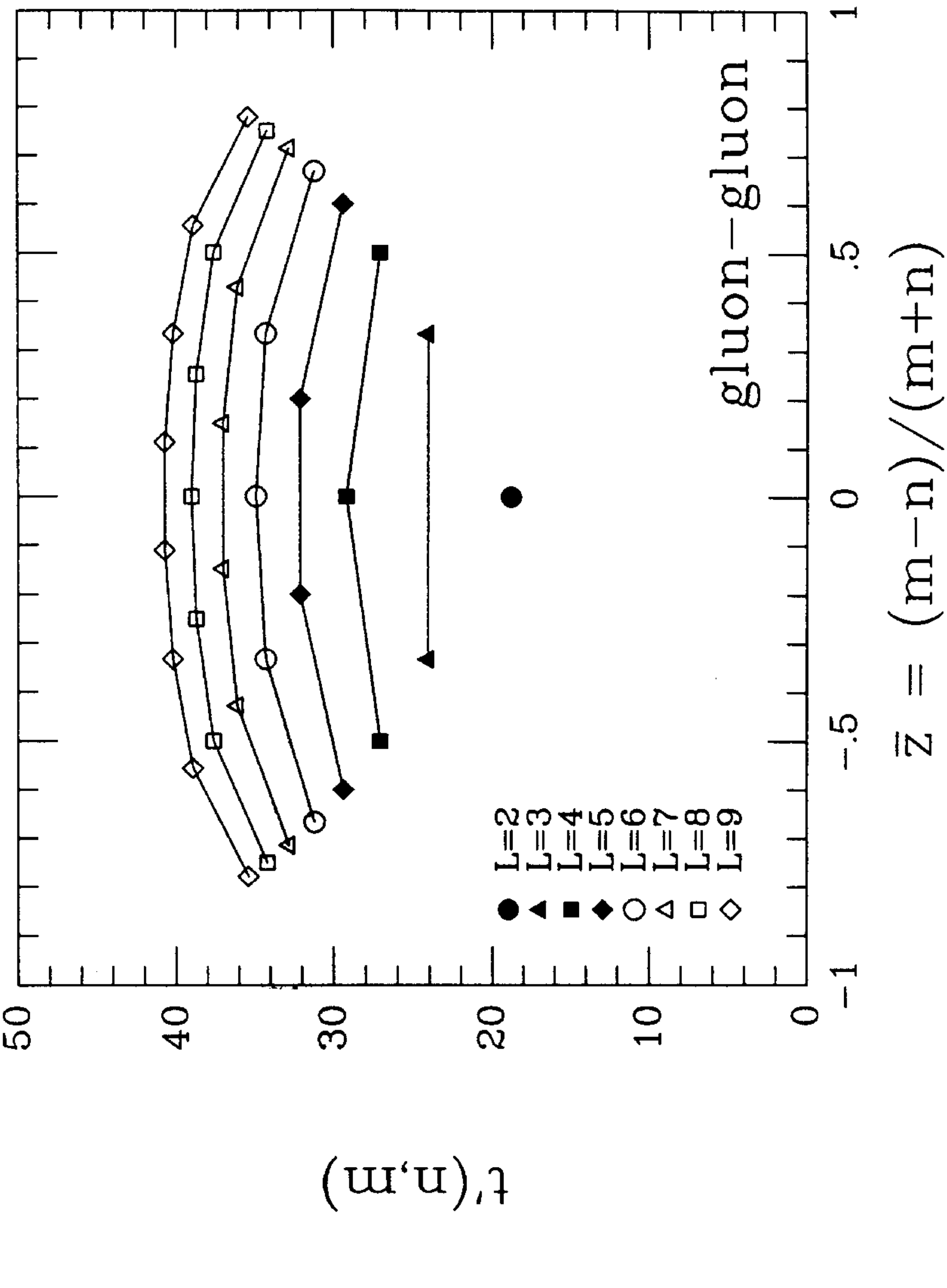

gluon−gluon
L=2
L=3
L=4
L=5
L=6
L=7
L=8
L=9
$\bar{z} = (m-n)/(m+n)$
t′(n,m)
−1
−.5
0
.5
1
0
10
20
30
40
50

FIGURE 16